Nuclear Physics B236 (1984) 269–310

ENERGY-ENERGY CORRELATIONS IN e^+e^- ANNIHILATION

A ALI

Deutsches Elektronen-Synchrotron DESY, Hamburg, Federal Republic of Germany

F BARREIRO

Universität Siegen, Siegen, Federal Republic of Germany

Received 11 August 1983
(Revised 28 October 1983)

We calculate energy-energy correlation (EEC) up to $O(\alpha_s)^2$ in perturbative QCD. The effects of heavy quark masses and experimental resolution in the spirit of Sterman-Weinberg on the EEC functions are also calculated to the same order. We find that the EEC function is sensitive to both the radiative corrections and experimental resolution criterion. The asymmetric EEC function is, in contrast, stable with respect to both the radiative and power corrections in perturbation theory. It is argued that both the data and perturbation theory indicate substantial non-perturbative power corrections to the EEC but modest effects in the asymmetry for $Q \geqslant 25$ GeV. We show that limited-p_T fragmentation models without long-range colour correlations are in agreement with the expectations and data. A phenomenological analysis of the PETRA/PEP data is performed to determine the QCD scale parameter. We determine $\Lambda_{\overline{MS}} = 120^{+60}_{-47}$ MeV with no power corrections, and $\Lambda_{\overline{MS}} = 168^{+60}_{-40}$ MeV if limited-p_T fragmentation effects are included. The small non-perturbative power correction to the asymmetric EEC is a characteristic feature of the limited-p_T independent parton-fragmentation models and is testable at PETRA energies.

1. Introduction

It is an increasingly popular idea that energy-energy correlation (EEC) provides a precision test of QCD at the ongoing experiments at PETRA/PEP energies. The EEC was introduced by Basham, Brown, Ellis and Love [1], who studied it in the first non-trivial order and showed that it is calculable in perturbative QCD, i.e. it is free of mass singularities. First measurements by the PLUTO collaboration [2] were encouraging. Since then the EEC has been calculated to order α_s^2 by the present authors [3] and by Richards, Stirling and Ellis [4] for the massless quarks and gluons. Recent measurements by the CELLO, MAC, MARK-J, and the MARK-II collaborations [5] involving high-statistics data have brought about the fine qualitative rapport of perturbative QCD and e^+e^- data, at the same time emphasizing the importance of power corrections for quantitative tests.

In this paper, we study questions which have a direct bearing on such comparisons and which in our opinion have to be answered for a quantitative test of QCD. In doing this, we shall elaborate on the results in ref. [3] and systematically study power corrections in perturbation theory (quark masses, resolution dependence) and from non-perturbative sources (fragmentation of quarks and gluons).

To recapitulate briefly, the EEC is a measurement of energy flow involving two calorimeters, subtending solid angles Ω and Ω' with respect to the incoming e^+e^- axis and having an angle χ between them. The quantity of interest to us is the "average" EEC obtained by keeping χ fixed and integrating over all other orientations. This can be regarded as the energy weighted sum over pairs of particles whose relative angle lies between χ and $\chi + \Delta\chi$,

$$\frac{1}{\sigma}\frac{\mathrm{d}\Sigma^{\mathrm{c}}}{\mathrm{d}\cos\chi} = \frac{2}{Q^2\,\Delta\chi\sin\chi}\frac{1}{N}\sum_{A=1}^{N}\sum_{\text{pairs}} E_a^A E_b^A, \tag{1.1}$$

a and b label individual particles and the normalization is

$$\int_{-1}^{1}\mathrm{d}\cos\chi\frac{1}{\sigma}\frac{\mathrm{d}\Sigma^{\mathrm{c}}}{\mathrm{d}\cos\chi} = 1 \tag{1.2}$$

when self-correlations ($a = b$, $\chi = 0°$) are included.

In perturbative QCD, the EEC receives contributions from the following processes:

$$\mathrm{e}^+\mathrm{e}^- \to \mathrm{q}\bar{\mathrm{q}}, \tag{1.3}$$

$$\to \mathrm{q}\bar{\mathrm{q}}\mathrm{G}, \tag{1.4}$$

$$\to \mathrm{q}\bar{\mathrm{q}}\mathrm{G}\mathrm{G}, \mathrm{q}\bar{\mathrm{q}}\mathrm{q}\bar{\mathrm{q}}. \tag{1.5}$$

Process (1.3) contributes at $\chi = 0°$ and 180° and the others contribute at all angles. If one is interested in measuring the EEC at angles $\chi \neq 0°$, 180°, one has to calculate only the processes (1.4) and (1.5) to $O(\alpha_s)^2$. For massless quarks and gluons this was calculated in refs. [3,4]. The results of the $O(\alpha_s)^2$ calculation can be expressed as

$$\frac{1}{\sigma_0}\frac{\mathrm{d}\Sigma^{\mathrm{c}}}{\mathrm{d}\cos\chi} = \frac{\alpha_s(Q^2)}{\pi}F(\xi) + \left(\frac{\alpha_s(Q^2)}{\pi}\right)^2 G(\xi),$$

$$\sigma_0 \equiv 4\pi\alpha^2/3Q^2\sum_f Q_f^2, \tag{1.6}$$

where $F(\xi)$ is the $O(\alpha_s)$ BBEL function [1]

$$F(\xi) = \frac{(3-2\xi)}{6\xi^5(1-\xi)}\left[2(3-6\xi+2\xi^2)\ln(1-\xi) + 3\xi(2-3\xi)\right], \tag{1.7}$$

with

$$\xi = \tfrac{1}{2}(1 - \cos\chi),$$

and $\alpha_s(Q^2)$ is given by the two-term Callan-Symanzik β function:

$$\alpha_s(Q^2) = 2\pi/\left[b_0 \ln(Q^2/\Lambda^2) + (b_1/b_0)\ln\ln(Q^2/\Lambda^2)\right], \tag{1.8}$$

with

$$b_0 = \tfrac{1}{6}(33 - 2n_f), \qquad b_1 = \tfrac{1}{6}(153 - 19n_f),$$

n_f being the number of quark flavours. In this paper we have used $n_f = 5$ and all $O(\alpha_s)^2$ quantities are calculated in the $\overline{\text{MS}}$ scheme [6].

A related quantity of interest is the asymmetric part of the EEC defined as [1]:

$$\frac{d\Sigma^A}{d\cos\chi} \equiv \frac{d\Sigma^c(180^\circ - \chi)}{d\cos\chi} - \frac{d\Sigma^c(\chi)}{d\cos\chi}. \tag{1.9}$$

In perturbative QCD this can be obtained from eq. (1.6). In conformity with our previous notation [3] we define the functions $A(\xi)$ and $B(\xi)$

$$\frac{1}{\sigma_0}\frac{d\Sigma^A}{d\cos\chi} = \frac{\alpha_s(Q^2)}{\pi}A(\xi) + \left(\frac{\alpha_s(Q^2)}{\pi}\right)^2 B(\xi), \tag{1.10}$$

where

$$A(\xi) = F(1-\xi) - F(\xi),$$

$$B(\xi) = G(1-\xi) - G(\xi). \tag{1.11}$$

The aim of this paper is to study the question, "how closely do the perturbative QCD results (1.6) and (1.10) represent the experimental measurements (1.1) and (1.9)?" Towards that end we have calculated the functions $G(\xi)$ and $A(\xi)$ more accurately and estimated power corrections to the EEC. These corrections include:

(i) quark mass effects;

(ii) experimental resolution dependence in the spirit of Sterman and Weinberg [7];

(iii) non-perturbative (fragmentation) contributions.

The origin of (i) and (iii) is intuitively clear but point (ii) perhaps needs some elaboration. It is well-known from QED that the radiative corrections are defined only for a given experimental setup. For example, one has to specify the minimum energy of the photon detectable in an experiment. The situation in QCD is not too different, though a great deal more complex due to confinement effects. We

systematically take into account the effect of experimental resolution on the underlying perturbative calculations for the EEC.

We use the Sterman-Weinberg variables $\varepsilon \equiv \min(E_i)/E_{c\,m}$ and $\delta = \min_{i\neq j}(\theta_{ij})$ and study the effect of (ε, δ) resolution on the perturbative function $F(\xi), G(\xi)$ and their asymmetric parts*. The cut on the angle δ means that the EEC is studied only for angles $\delta < \chi < 180° - \delta$. In other words the back-to-back configurations with $\chi \simeq 180°$ or almost collinear configuration with $\chi \simeq 0°$ no longer are accessible in fixed-order perturbation theory. The cut on ε simply removes the soft partons from the EEC.

The SW-resolution criterion serves two purposes. Firstly, it is generally accepted that the non-perturbative effects dominate for $\chi = 0°$ and 180° and so the use of fixed-order perturbation theory in this region is not very advisable. Secondly, and more importantly, this criterion provides a systematic way to judge which of the perturbative distributions, or parts thereof, are infrared stable.

We go a step further in this paper and advocate that the SW-resolution criterion, though strictly a perturbative artifact and in fact invented precisely because we do not know the complete theory, could be used to guess the relative importance of non-perturbative (fragmentation) effects. Of course, it assumes that the quantity being investigated is factorizable, i.e. it is calculable in perturbation theory. We elaborate this point in the example of EEC and to keep the argument simple we first concentrate on the leading non-trivial order. The EEC for the process (1.4) defined with the SW criterion is given by

$$\frac{1}{\sigma_0}\frac{\mathrm{d}\Sigma^{c}(\varepsilon,\delta)}{\mathrm{d}\cos\chi} = \frac{\alpha_s(Q^2)}{\pi}F(\xi,\varepsilon), \qquad \delta < \chi < 180° - \delta. \tag{1.12}$$

We have computed in sect. 2 the function $F(\xi, \varepsilon)$ and the result can be expressed as

$$F(\xi,\varepsilon) = F(\xi) - \tfrac{2}{3}\varepsilon\frac{1}{\xi(1-\xi)} + \frac{\varepsilon^2(3-2\xi)}{6\xi(1-\xi)} + \mathrm{O}(\varepsilon)^3, \tag{1.13}$$

where $F(\xi)$ is given in eq. (1.6). Note that the SW criterion results in power corrections ($\varepsilon = \min E_i/Q$) and the dependence of $F(\xi, \varepsilon)$ on ε is linear. Hence the perturbative QCD distribution for the EEC is sensitive to the soft-parton contribution. Based on this criterion, we expect substantial contributions from non-perturbative effects and this indeed is the case experimentally [5].

* It will become clear that the soft energy cut in our calculations is the same as in the Sterman-Weinberg prescription However, the cut on the angle has a different interpetation in the EEC, namely that the perturbation theory weights for the 3- and 4-parton processes are evaluated only from the angular configurations $\chi > \delta$ Thus, it would be more appropriate to call our cuts (ε, χ) cuts We hope that this does not cause any confusion

The (ε, δ) dependent asymmetric part of the EEC can be calculated from

$$\frac{1}{\sigma_0}\frac{\mathrm{d}\Sigma^A(\varepsilon,\delta)}{\mathrm{d}\cos\chi} = \frac{\alpha_s(Q^2)}{\pi}A(\xi,\varepsilon)\theta(\chi-\delta), \tag{1.14}$$

with

$$A(\xi,\varepsilon) = A(\xi) + \frac{\varepsilon^2(2\xi-1)}{3\xi(1-\xi)} + \mathrm{O}(\varepsilon)^3. \tag{1.15}$$

Note that the power corrections to $A(\xi, \varepsilon)$ vanish quadratically with ε and hence the asymmetric part of the EEC is relatively stable in $\mathrm{O}(\alpha_s)$. It is curious, and we believe not quite accidental, that the data for the asymmetric EEC cross section also requires small non-perturbative contributions. Moreover, the Q dependence of the asymmetric cross section at PETRA for $\chi > 30°$ is very mild. In sect. 3 we show that limited-p_T fragmentation models *without* any additional correlations are also qualitatively in agreement with the perturbative result (1.13) and (1.15) i.e. they lead to substantial non-perturbative contributions to EEC but give rise to modest effects in the asymmetry.

There is yet another source of power corrections, which is exactly calculable in perturbative QCD, namely the quark mass effects. We take them into account in the Born diagrams for the process (1.4) and (1.5). Even though the c.m. energy where most of the PETRA/PEP data is taken lies substantially above the charm and bottom quark-pair production threshold, the effect on the EEC is still about 10%. The redeeming feature of this is that the comparison of perturbative QCD calculations with the data results in rather reasonable description of the asymmetry, and yields a value of $\Lambda_{\overline{\mathrm{MS}}}$ consistent with the generally anticipated values for this quantity.

The paper is organized as follows. In sect. 2 we present a recalculation of the EEC functions $G(\xi)$ and $B(\xi)$ for massless quarks and gluons. Our results are compared to those of ref. [4] and they are found to be compatible with those in ref. [4] within calculational errors. We give a simple parametrization for the function $R^{\mathrm{corr}}(\xi)$ (related to $G(\xi)$) based on a fit of our numerical computation of the same quantity. The effect of the SW resolution on the functions $F(\xi)$ and $G(\xi)$ is evaluated. Again, we give a parametrization for the function $R^{\mathrm{corr}}(\xi, \varepsilon)$ for some representative values of ε and δ. Next, we calculate the effect of quark masses on the functions $F(\xi, \varepsilon)$ and $G(\xi, \varepsilon)$. Within our calculational errors, we find the dependence of the $\mathrm{O}(\alpha_s)$ and $\mathrm{O}(\alpha_s)^2$ terms on quark masses very similar and both are proportional to m/E_{CM}. The information in sect. 2 is sufficient to make a comparison of data on the EEC with perturbative QCD in the second order.

In sect. 3 we estimate non-perturbative fragmentation effects on the EEC cross section. This estimate is based on the use of limited-p_T fragmentation models incorporating independent fragmentation of quarks and gluons in the processes (1.3)–(1.5). Not unexpectedly, the asymmetric EEC cross section from the process

$q\bar{q} \to$ hadrons falls off exponentially with χ and $\sqrt{s}$. So, for $\sqrt{s} \geqslant 30$ GeV, $\chi \geqslant 30°$, $q\bar{q} \to$ hadrons gives no contributions in $\Sigma^A(\chi)$. It is shown that the fragmentation contribution to $\Sigma^A(\chi)$ in such models has a shape very similar to the perturbative EEC. The normalization is obtained by fixing the p_T and p_L distributions of hadrons at PETRA energies. Typically, the fragmentation contribution at $\sqrt{s} = 30$–35 GeV in these models is $\sim 15\%$ and it falls off like $1/\sqrt{s}$. We provide a simple parametrization for Σ^A_{frag}, valid for $\sqrt{s} \geqslant 20$ GeV. This is only weakly correlated with the intrinsic p_T of the hadrons or on the details of the p_L distribution of hadrons from quarks or gluons.

In sect. 4 we compare the complete $O(\alpha_s)^2$ calculation with the data, both including the fragmentation effects of sect. 3 and without. We find that $d\Sigma^A(\chi)$ from the perturbation theory is in remarkable agreement with the data. We use the asymmetry at large angles $\chi \geqslant 30°$ and it gives $\Lambda_{\overline{\text{MS}}} = 120^{+60}_{-40}$ MeV. We remark that this is a *lower bound* on $\Lambda_{\overline{\text{MS}}}$. Including non-perturbative contribution increases the $\alpha_s(Q^2)$ by $\sim 15\%$ resulting in $\alpha_s(Q) = 0.13 \pm 0.01$ yielding $\Lambda_{\overline{\text{MS}}} = 168^{+60}_{-40}$ MeV. This is in remarkable agreement with the world-average $\Lambda_{\overline{\text{MS}}} = 160^{+100}_{-80}$ MeV [8]. We further remark that the fragmentation contribution is testable at presently available PETRA energies and we advocate an energy dependent study of $\Sigma^A(\chi)$ to independently determine the power corrections from the data. The power corrections are measurably different in models with and without long-range colour correlations.

Sect. 5 contains our conclusions.

2. Perturbative QCD calculation of EEC

In this section we present the results for the perturbative QCD calculation of the processes (1.4) and (1.5) to order α_s^2. A representative sampling of the relevant Feynman diagrams is shown in fig. 1. We start by deriving first the $O(\alpha_s)$ EEC in a

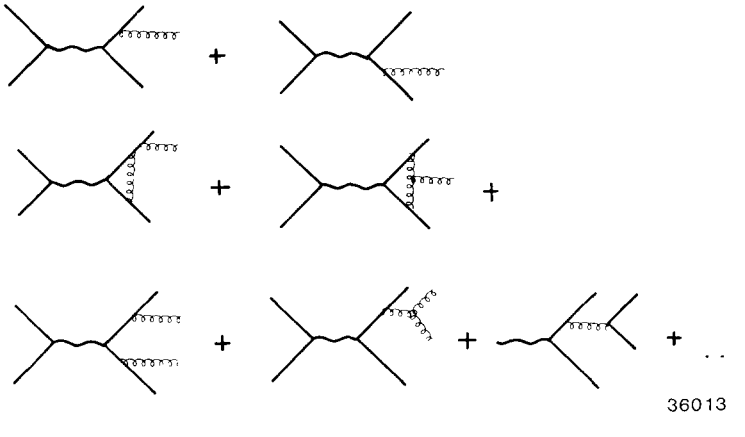

Fig 1 A sampling of the $O(\alpha_s)$ and $O(\alpha_s)^2$ Feynman diagrams in e^+e^- annihilation into hadrons

somewhat different form than has been done in ref. [1]. This is being undertaken to present our calculational method in a simple form for subsequent derivations.

The $O(\alpha_s)$ EEC can also be expressed as

$$\frac{1}{\sigma_0}\,\mathrm{d}\Sigma^{c} = \frac{\alpha_s(Q^2)}{\pi} C_F \int \mathrm{d}y_{12}\,\mathrm{d}y_{23}\,\mathrm{d}y_{13}\,\delta(1-y_{12}-y_{23}-y_{13})\tilde{T}, \tag{2.1}$$

where

$$\tilde{T} = \sum_{i,j} \frac{2E_iE_j}{Q^2}\delta(\chi-\theta_{ij})T(y_{12}, y_{13}, y_{23}),$$

and T is the density for the process $e^+e^- \to q\bar{q}G$ derived by Ellis, Gaillard and Ross [9]:

$$T(y_{12}, y_{13}, y_{23}) = \frac{y_{13}}{y_{23}} + \frac{y_{23}}{y_{13}} + \frac{2y_{12}}{y_{13}y_{23}},$$

$$y_{ij} = s_{ij}/Q^2, \qquad s_{ij} = (p_i + p_j)^2. \tag{2.2}$$

By a suitable transformation one could write eq. (2.1) in the form

$$\frac{1}{\sigma_0}\frac{\mathrm{d}\Sigma^{c}}{\mathrm{d}\cos\chi} = \frac{1}{8}\frac{\alpha_s(Q^2)}{\pi} C_F \int \mathrm{d}y\,(\omega+1)^3 \frac{(1-y)^2}{y^3} z^2[T_{12}+2T_{13}], \tag{2.3}$$

where

$$T_{12} = \frac{1-y}{y}\frac{\omega}{z} + \frac{y}{1-y}\frac{z}{\omega} + \frac{2}{\omega},$$

$$T_{13} = \frac{1-y}{y} + \frac{y}{1-y} + 2\frac{\omega}{z^2},$$

$$z = 1-(1+\omega)(1-y), \qquad \omega = \xi/(1-\xi), \qquad y = 1-\frac{2E_1}{Q}\xi. \tag{2.4}$$

Eq. (2.3) involves a simple integral, which can be done in a straightforward way and one obtains

$$\frac{1}{\sigma_0}\frac{\mathrm{d}\Sigma^{c}}{\mathrm{d}\cos\chi} = \frac{1}{8}\frac{\alpha_s(Q^2)}{\pi} C_F[g_{12}(\xi) + 2g_{13}(\xi)], \tag{2.5}$$

where

$$g_{12}(\xi) = \frac{(\omega+1)^3}{3\omega}\left[-17-42\omega-24\omega^2-6(\omega+1)^2(4\omega+1)\ln\frac{\omega}{\omega+1}\right],$$

$$2g_{13}(\xi) = \frac{(\omega+1)^3}{3\omega}\left[8+33\omega+78\omega^2+6\omega(3+12\omega+13\omega^2)\ln\frac{\omega}{\omega+1}\right]. \quad (2.6)$$

Using the relation $\omega = \xi/(1-\xi)$ and $C_F = \frac{4}{3}$ one immediately obtains the $O(\alpha_s)$ BBEL formula

$$\frac{1}{\sigma_0}\frac{d\Sigma^c}{d\cos\chi} = \frac{\alpha_s(Q^2)}{\pi}F(\xi), \quad (2.7)$$

where $F(\xi)$ is given in eq. (1.7). There are several comments that we would like to make here about the derivation (2.1)–(2.7).

(i) In order to calculate the $O(\alpha_s)^2$ effects to the EEC for the 3-parton state one has to cast the results in the form of eq. (2.1) i.e. one has to derive the density $\tilde{T}$ to the desired order by including the real and virtual diagrams and integrating out all other variables up to the double-differential Dalitz distribution.

(ii) The experimental resolution i.e. a cut on the SW parameters ε and δ can be imposed on the Dalitz boundaries whose parametric equation is given by the argument of the delta function in (2.1).

(iii) The fact that $g_{12}(\xi) \neq 2g_{13}(1-\xi)$ is the reason why the asymmetric EEC function $A(\xi)$ is not zero.

We shall now calculate the EEC in order α_s^2. This will be done in two ways. First we present our results for the case $\varepsilon = \delta = 0$. This is the limit in which Ellis, Ross and Terrano (ERT) [10] calculated the $O(\alpha_s)^2$ corrections to the Fox-Wolfram shape parameters [11]. The order α_s^2 calculations for the EEC reported in refs. [3,4] were also done in this limit. Then we shall discuss the case of finite (ε, δ) resolution-dependent $O(\alpha_s)^2$ corrections. This is the spirit in which Fabricius, Schmitt, Schierholz and Kramer [12] have done the $O(\alpha_s)^2$ radiative corrections. Since the difference between the two approaches lies in terms which are essentially power corrections, doing the $O(\alpha_s)^2$ radiative corrections in two ways provides a systematic account of those power corrections which have a perturbative origin. In fact the stability of a jet measure with respect to the experimental resolution is a reasonable criterion of reliability for perturbation theory results. This is so because the direct one-to-one correspondence between experimental and theoretical resolutions, to which we are accustomed from QED radiative corrections, is clouded by non-perturbative confinement effects.

2.1 EEC WITH INFINITE EXPERIMENTAL RESOLUTION

Starting the $\varepsilon = \delta = 0$ calculations, we have made use of the ERT results [10] on virtual correction to $e^+e^- \to q\bar{q}G$, which we find particularly useful in calculating

the EEC. As remarked earlier one needs $\tilde{T}$ to $O(\alpha_s)^2$ from which the virtual $O(\alpha_s)^2$ correction to the EEC can be calculated as shown in the derivation (2.1)–(2.6). Following the derivation of the $O(\alpha_s)$ BBEL formula, using the formula for T from ERT, eq. (3.26) of the second ref. in [10], and after some straightforward algebra, one can derive the virtual $O(\alpha_s)^2$ contribution to the EEC. The result is

$$\frac{1}{\sigma}\frac{d\Sigma^c_{vir}}{d\cos\chi} = \frac{1}{8}\frac{\alpha_s(Q^2)}{\pi}C_F\Bigg[6F(\xi) + \frac{\alpha_s(Q^2)}{\pi}\Bigg\{ g_{12}(\xi)\big[C_F\big(\tfrac{2}{3}\pi^2 - 1 - \ln^2\omega - \tfrac{3}{2}\ln\omega\big)$$

$$+ N_c\big(\tfrac{1}{3}\pi^2 + \tfrac{67}{18} - \tfrac{11}{6}\ln\omega\big) + T_R\big(\tfrac{2}{3}\ln\omega - \tfrac{10}{9}\big)\big]$$

$$+ 2g_{13}(\xi)\big[C_F\big(\tfrac{2}{3}\pi^2 - 1 - 3\ln\omega\big) + N_c\big(\tfrac{1}{3}\pi^2 + \tfrac{67}{18} - \ln^2\omega\big) - \tfrac{10}{9}T_R\big]$$

$$+ (\omega+1)^3\int_{(\omega/\omega+1)}^{1} dy\,\frac{(1-y)^2}{y^3}z^2T_v(\omega, y)\Bigg\}\Bigg], \tag{2.8}$$

where the function $T_v(\omega, y)$ is given in appendix A. The $O(\alpha_s)^2$ piece in eq. (2.8) is the sum of the virtual 3-parton and the real 4-parton contribution. We recall that the real 4-parton singular piece is obtained by treating the event as a quasi 3-parton state when one of the invariant masses $y_{ij} = s_{ij}/Q^2$ goes to zero, with $y_{ijk} = (p_i + p_j + p_k)^2/Q^2$ and y_{ijl} held fixed. This is explained in detail in the ERT papers [10] to which we refer for the precise prescription. Alternatively, one could use the pole terms due to Kunzst [13], involving an invariant mass cut-off $y_{min} = \min(m_J^2/Q^2, y_{ijk}, y_{ijl})$ where m_J is some pre-defined jet mass. The corresponding expression for $d\Sigma^c_{vir}$ then differs from eq. (2.8). However, this difference is *exactly* compensated by the finite 4-parton piece. Eq. (2.8) involves a one-dimensional integral which could be done to any arbitrary accuracy. We have used a (double precision) NAGLIB subroutine which does the integral using a gaussian quadrature method and we stopped at an accuracy of 1 part in 10^6.

The finite 4-parton piece was obtained numerically by calculating the 4-body phase space using a Monte Carlo technique. Symbolically one can write this contribution as

$$\frac{1}{\sigma}\frac{d\Sigma^c_{real}}{d\cos\chi} = \int(d4)\Sigma^{(4)}T^{(4)} - \int(\overline{d4})\bar{\Sigma}^{(4)}\bar{T}^{(4)}, \tag{2.9}$$

where $T^{(4)}$ is the matrix-element squared for the 4-parton processes (1.5) and $\bar{T}^{(4)}$ is the y_{ij}^{-1} piece of it, which has been integrated analytically and included in eq. (2.8). (This is the reason why $\bar{T}^{(4)}$ has to be subtracted as in (2.9) to get the finite $d\Sigma^c_{real}$.) Since the quantity on the right-hand side of eq. (2.9) is by construction finite, one

needs $T^{(4)}$ and $\bar{T}^{(4)}$ in the physical space-time dimensions. The expressions for $T^{(4)}$ are given in refs. [14, 15] for the general case of non-zero quark masses, as well as by ERT, who have worked in the limit $m = 0$. The expression for $\bar{T}^{(4)}$ is given by ERT*. See also the appendix of ref. [4]. Note that the bar on d4 in the second term of eq. (2.9) means that the phase space in the second integral is *different* from the complete 4-body phase space and it is this piece which keeps track of different procedures in defining the virtual 4-parton cross sections. We emphasize that since $\bar{T}^{(4)}$ involves only the y_{ij}^{-1} pole pieces (and *not* the complete expression for $T^{(4)}$ in the limit $y_{ij} \to 0$), one has in general a *non-zero* contribution for the left-hand side of eq. (2.9) in the kinematic domain defined by $(\overline{\mathrm{d4}})$. Numerically, we find that this contribution, which in the jargon is also referred to as the soft 4-parton contribution, is not negligible. In particular, for the pole-terms, used by ERT, the contribution for the EEC from the soft 4-jet piece is *not* simply proportional to a power of the angle.

We make the obvious remark that the use of Monte Carlo integration techniques allows us to impose any experimental resolution that one would like to impose by redefining the phase space. Thus, it is a simple matter for example to go to the FSSK limit in calculating (2.9), or impose the Sterman-Weinberg resolution on EEC.

The complete $O(\alpha_s)^2$ corrections to the EEC are given by the sum of eqs. (2.8) and (2.9). In conformity with the notation used in ref. [3] we present our result first in the form of eq. (1.6):

$$\frac{1}{\sigma_0}\frac{\mathrm{d}\Sigma^c}{\mathrm{d}\cos\chi} = \frac{\alpha_s(Q^2)}{\pi}F(\xi) + \left(\frac{\alpha_s(Q^2)}{\pi}\right)^2 G(\xi).$$

The values of $F(\xi)$ and $G(\xi)$ are given in table 1. Note that since we are using a Monte Carlo integration technique to calculate $\mathrm{d}\Sigma^c$, the values of the F and G functions are averages in the $\cos\chi$ bin with a width $\Delta\cos\chi = 0.1$. A typical error in the $O(\alpha_s)^2$ function $G(\xi)$ is $\pm 4\%$. Thus, the EEC cross section is calculated to an accuracy of $\pm 1\%$. Since the systematic errors in experimental measurements overwhelm our calculational accuracy, we think that an error $\pm 1\%$ in Σ^c is adequate for our analysis. We have generated $\sim 10^7$ Monte Carlo events and the 4% inaccuracy in G is a remnant of the subtraction in the integrand of eq. (2.9).

Instead of presenting our result in the form of eq. (1.6), which is normalized with respect to the point-like cross section σ_0, one could normalize the correlation cross section to σ, calculated to order α_s^2, which then guarantees to $O(\alpha_s)^2$ the normalization eq. (1.2). Rewriting eq. (1.6) one has now

$$\frac{1}{\sigma}\frac{\mathrm{d}\Sigma^c}{\mathrm{d}\cos\chi} = \frac{\alpha_s(Q^2)}{\pi}F(\xi)\left[1 + \frac{\alpha_s(Q^2)}{\pi}R^{\mathrm{corr}}(\xi)\right], \tag{2.10}$$

* Strictly speaking it is the y_{ij}^{-1} piece of the matrix-element squared integrated up to the trivial angular orientations

where σ is the total hadronic cross section in the $\overline{\text{MS}}$ scheme [16]:

$$\sigma = \sigma_0\left(1 + \frac{\alpha_s(Q^2)}{\pi} + c_2\left(\frac{\alpha_s(Q^2)}{\pi}\right)^2\right), \tag{2.11}$$

where

$$c_2 = (1.98 - 0.116 n_f) = 1.40 \quad \text{for} \quad n_f = 5.$$

The values of $R^{\text{corr}}(\xi)$ are given in table 2 (column 2). We remark that $R^{\text{corr}}(\xi)$ depends on the angle χ, increasing from about 7 for $\cos\chi = -0.85$ to about 10 at $\cos\chi = +0.85$. Thus in the central region, order $(\alpha_s)^2$ corrections to the BBEL function $F(\xi)$ are substantial. Consequently the value of α_s extracted from the EEC cross section can differ by about (30–40)% in the first and second order.

Next we would like to present a simple parametrization for the function $R^{\text{corr}}(\xi)$. An acceptable fit to $R^{\text{corr}}(\xi)$ is obtained using the expression

$$R^{\text{corr}}(\xi) = -\tfrac{2}{3}\ln^2(1/[1-\xi]) + A\ln(1/[1-\xi]) + B + C\xi, \tag{2.12}$$

TABLE 1
The BBEL $F(\xi)$ and the $O(\alpha_s)^2$ function $G(\xi)$ defined for the EEC cross sections in eq (1.6) for the massless quark and gluon case without experimental resolution

$\cos\chi$ (interval)	$F(\xi)$	$G(\xi)_{\text{calculated}}$	$G(\xi)_{\text{fitted}}$
−0.90, −0.80	8 751	62.43 ± 1.89	61.86
−0.80, −0.70	4 464	35.12 ± 1.21	33.62
−0.70, −0.60	2 975	21.81 ± 0.87	23.17
−0.60, −0.50	2 251	16.37 ± 0.76	17.97
−0.50, −0.40	1 838	14.12 ± 0.87	15.00
−0.40, −0.30	1 581	13.40 ± 0.57	13.17
−0.30, −0.20	1 413	12.79 ± 0.72	12.03
−0.20, −0.10	1 304	11.47 ± 0.52	11.34
−0.10, 0.00	1 235	11.08 ± 0.40	10.99
0.00, 0.10	1 199	10.26 ± 0.57	10.91
0.10, 0.20	1 192	11.22 ± 0.43	11.09
0.20, 0.30	1 214	11.34 ± 0.42	11.55
0.30, 0.40	1 269	13.28 ± 0.43	12.37
0.40, 0.50	1 370	14.07 ± 0.54	13.66
0.50, 0.60	1 540	15.87 ± 0.47	15.71
0.60, 0.70	1 833	19.45 ± 0.64	19.14
0.70, 0.80	2 395	25.98 ± 0.72	25.60
0.80, 0.90	3 805	38.50 ± 1.20	41.63

$G(\xi)_{\text{fitted}}$ is the result of fitting $G(\xi)_{\text{calculated}}$ using the parametrization of eq (2.12)

TABLE 2
The $O(\alpha_s)^2$ EEC function $R^{corr}(\xi)$ defined in eq (2 10) for the massless quark and gluon case both with and without experimental resolution

cos χ	$R_{corr}(\cos\chi)$	$R^{fit}_{corr}(\cos\chi)$	R^{fit}_{corr} ε = 5%	R^{fit}_{corr} ε = 10%	R^{fit}_{corr} ε = 15%
−0 90, −0 80	7 13 ± 0 21	7 06	9 83	9 00	6 93
−0 80, −0 70	7 86 ± 0 27	7 53	9 69	9 24	8 35
−0 70, −0 60	7 33 ± 0 29	7 78	9 68	9 40	9 24
−0 60, −0 50	7 27 ± 0 34	7 98	9 77	9 60	9 67
−0 50, −0 40	8 12 ± 0 47	8 15	9 94	9 83	10 07
−0 40, −0 30	8 47 ± 0 36	8 33	10 17	10 10	10 38
−0 30, −0 20	9 05 ± 0 51	8 51	10 48	10 40	10 64
−0 20, −0 10	8 79 ± 0 40	8 70	10 77	10 72	10 86
−0 10, 0 00	8 96 ± 0 32	8 89	11 12	11 06	11 06
0 00, 0 10	8 55 ± 0 47	9 09	11 50	11 43	11 24
0 10, 0 20	9 41 ± 0 36	9 30	11 91	11 81	11 41
0 20, 0 30	9 34 ± 0 35	9 51	12 34	12 20	11 56
0 30, 0 40	10 46 ± 0 34	9 34	12 78	12 61	11 71
0 40, 0 50	10 27 ± 0 39	9 97	13 25	13 03	11 85
0 50, 0 60	10 30 ± 0 30	10 20	13 73	13 46	11 99
0 60, 0 70	10 61 ± 0 35	10 44	14 22	13 90	12 12
0 70, 0 80	10 84 ± 0 30	10 68	14 72	14 35	12 24
0 80, 0 90	10 11 ± 0 31	10 93	15 24	14 81	12 37

Column (ii) $R^{corr}_{calculated}$ ($\varepsilon = \delta = 0$), column (iii) R^{corr}_{fitted} ($\varepsilon = \delta = 0$) using the parametrization of eq (2 12), (iv) R^{corr} ($\varepsilon = 0\,05, \delta = 26°$), (v) R^{corr} ($\varepsilon = 0\,1, \delta = 26°$), (vi) R^{corr} ($\varepsilon = 0\,15, \delta = 26°$)

with

$$A = 3.0 \pm 0.3, \qquad B = +11.3 \pm 0.2, \qquad C = -8.2 \pm 0.9. \tag{2.13}$$

The parametrization eq. (2.12) correctly takes into account the leading-log structure. We have fixed the leading-log coefficient which has been calculated for $\chi \simeq 180°$ in ref. [17] and which we have verified numerically. The leading-log coefficient has also been verified in ref. [4]. In table 2 we show $R^{corr}(\xi)$ using eq. (2.12).

Once we have the functions $F(\xi)$ and $G(\xi)$ (or equivalently $R^{corr}(\xi)$) we can determine the asymmetric part of the EEC cross section as shown in eqs. (1.10) and (1.11). From now on we shall work with the fitted EEC function $R^{corr}(\xi)$ and compute all other functions related to it using the parametrization (2.12) and (2.13). In fig. 2 we plot the functions $F(\xi)$, $G(\xi)$ and in fig. 3 the corresponding asymmetric EEC functions $A(\xi)$ and $B(\xi)$. Note that the function $B(\xi)$ differs from our published result in ref. [3] in the large-χ region.

Just as we have done for the EEC cross section, we can define the asymmetric EEC functions which are normalized with respect to the total hadronic cross section

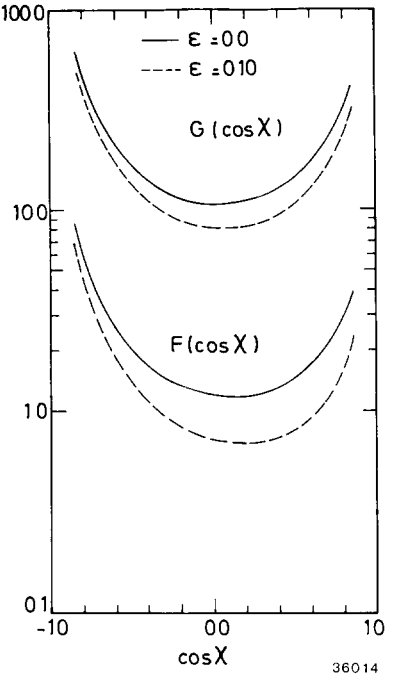

Fig 2 The $O(\alpha_s)$ and $O(\alpha_s)^2$ EEC functions defined in eq (1 6) The solid curves correspond to the case $\epsilon = \delta = 0$ and the dashed curves correspond to using $\epsilon = 0\,1$ and $\delta = 26°$ Note that $\epsilon = \min(E_i/\sqrt{s})$ and $\delta = \min(\theta_{ij})$

in the $\overline{\text{MS}}$ scheme:

$$\frac{1}{\sigma}\frac{d\Sigma^A}{d\cos\chi} = \frac{\alpha_s(Q^2)}{\pi}A(\xi)\left[1 + \frac{\alpha_s(Q^2)}{\pi}R^{\text{asym}}(\xi)\right], \tag{2.14}$$

with

$$R^{\text{asym}}(\xi) = R^{\text{corr}}(\xi) + \frac{F(1-\xi)}{A(\xi)}\left[R^{\text{corr}}(1-\xi) - R^{\text{corr}}(\xi)\right]. \tag{2.15}$$

In fig. 4 we plot the functions $R^{\text{corr}}(\xi)$ and $R^{\text{asym}}(\xi)$ and compare them with the corresponding functions obtained by Richards, Stirling and Ellis in ref. [4]. The two calculations are in fair agreement with each other*. Note that $R^{\text{asym}}(\xi)$ is a monotonously decreasing function of the angle χ and typically $R^{\text{asym}}(\xi) \simeq 3$. Thus

* Our values for $R^{\text{corr}}(\chi)$ though lie systematically higher by ~ 1 unit The results for $R^{\text{asy}}(\chi)$ are closer and hence both the calculations should lead to similar values for α_s

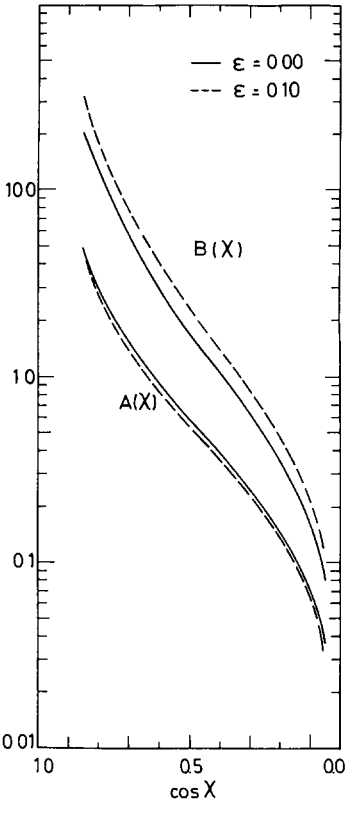

Fig 3 The $O(\alpha_s)$ and $O(\alpha_s)^2$ functions for the asymmetry in the EEC defined in eq (1.10) The notation used is the same as in fig 2

the $O(\alpha_s)^2$ corrections in the asymmetric EEC are small. The determination of $\alpha_s(Q)$ using the first and second order perturbative QCD calculations then would differ by $\sim 15\%$, with $\alpha_s[2] < \alpha_s[1]$.

The calculation of the perturbative QCD EEC functions reported in this subsection were done for the ideal case i.e. for infinite experimental resolution. Since the BBEL EEC function $F(\xi)$ is also defined with infinite experimental resolution, it was logical to calculate radiative corrections to it in the same limit i.e. with $\varepsilon = \delta = 0$. The idea was to show that calculating the radiative corrections à la ERT, the *size of the $O(\alpha_s)^2$ corrections depends on the measure*. In the example of EEC, the corrections are substantial for the correlation function itself but small for its asymmetric part. In subsect. 2.2 we study the effect of experimental resolution on the EEC and its asymmetry. Strictly speaking, these are perturbative power corrections as we shall presently see.

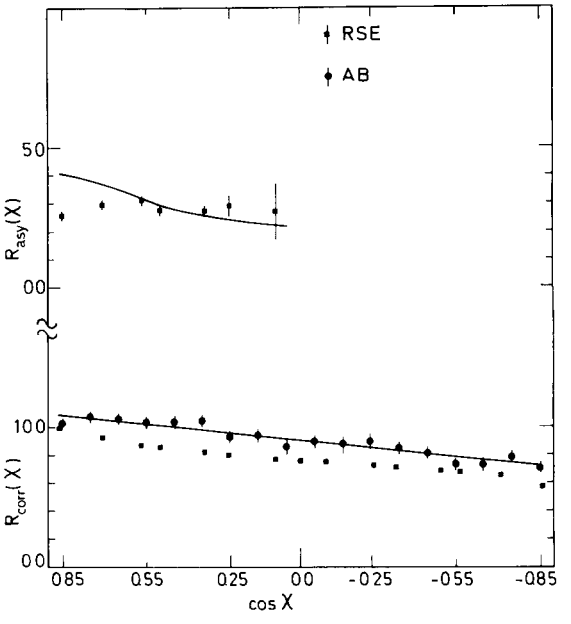

Fig 4 The $O(\alpha_s)^2$ EEC functions $R^{corr}(\xi)$ and $R^{asym}(\xi)$ as defined in eqs (2 10) and (2 14) respectively The solid lines are the fits using eq (2 12) The points denoted as □ are the results from Richards, Stirling and Ellis (second of ref [4], $n_f = 5$ case)

2 2 EEC WITH STERMAN-WEINBERG RESOLUTION

The idea is to define a resolution à la Sterman-Weinberg *first* and then calculate the EEC cross section. This procedure gives an angular width to a parton, and it defines when soft quanta are not resolvable. Since the effect of non-perturbative fragmentation is qualitatively similar, i.e. it gives an angular width to a parton, the perturbative resolution criterion may provide us with a guide about the reliability of a jet measure.

In order to avoid any misunderstanding let us state that we are making a distinction here between the *calculability* of a measure and its *reliability* as a precision test of perturbative QCD. The EEC function is calculable in perturbation theory up to at least $O(\alpha_s)^2$ i.e. it is free of any mass singularities and we have just shown that in subsect. 2.1. There is an impressive list of cross sections and distributions which have been shown to be free of mass singularities and hence by definition calculable. This list includes in addition to the EEC cross section, thrust distribution, the Fox-Wolfram shape parameters and many more. By *reliably calculable* we mean that a measure is not very sensitively dependent on the resolution of soft and collinear quanta. Since QCD is a confining theory, such a criterion is necessary to compare perturbative QCD calculations with data.

We shall use the Sterman-Weinberg variables $\varepsilon \equiv \min(E_i)/E_{c.m.}$ and $\delta = \min(\theta_{ij})$ to define whether or not a certain kinematic configuration is to be taken into account in the definition of genuine 3- and 4-jet events. We start by considering again the $O(\alpha_s)$ EEC function. Recall the definition of the EEC from eq. (2.1). The sum in the definition of the function $\tilde{T}$ runs over the pairs "12" ($q\text{-}\bar{q}$), "13" (q-g) and "23" ($\bar{q}$-g) for $\chi \neq 0°$, 180°. Thus, the angular cut δ can be implemented by the modification

$$\tilde{T}(\delta) = \sum_{i,j} 2\frac{E_i E_j}{Q^2} T(y_{12}, y_{13}, y_{23})\, \delta(\chi - \theta_{ij})\theta(\theta_{ij} - \delta). \tag{2.16}$$

To avoid any possible confusion we state that eq. (2.16) is the *definition* of our angular resolution in the EEC function. The resolution in energy for the 3-parton state is defined as follows. If for a given event the scaled energy, $E_i/\sqrt{s}$, of the least energetic parton is less than a preassigned cut ε, then the event is classified as a 2-parton event and its contribution is not included in $\tilde{T}(\delta)$. Later, we shall generalize these (ε, δ) prescriptions to a 4-parton state.

The ε-cut can be imposed on the Dalitz boundary in a straightforward manner. We explain it here for the configuration $i = 1$ and $j = 3$. In that case the integrals in (2.1) can be transformed to the variables E_1, E_3 and $\cos\chi$ by using the standard jacobian

$$\begin{aligned} &\mathrm{d}y_{12}\,\mathrm{d}y_{13}\,\mathrm{d}y_{23}\,\delta(1 - y_{12} - y_{13} - y_{23}) \\ &\quad = J\,\mathrm{d}E_1\,\mathrm{d}E_3\,\mathrm{d}\cos(\chi)\,\delta\left(E_3 - \frac{Q^2 - 2QE_1}{2(E_1\cos\chi + Q - E_1)}\right), \end{aligned} \tag{2.17}$$

where

$$J = \frac{4E_1E_3}{Q^2}\,\frac{1}{Q - E_1(1 - \cos\chi)},$$

and the variables y_{ij} are given by

$$\begin{aligned} y_{12} &= 2E_1/Q^2\left[Q - E_3(1 - \cos\chi)\right], \\ y_{13} &= 2E_1E_3/Q^2(1 - \cos\chi), \\ y_{23} &= 2E_3/Q^2\left[Q - E_1(1 - \cos\chi)\right]. \end{aligned} \tag{2.18}$$

The double-differential (Dalitz) distribution $\mathrm{d}^2\Sigma/\mathrm{d}E_1\,\mathrm{d}\cos\chi$ has the boundary given by the argument of the delta function in (2.17),

$$E_1 = \left(Q^2 - 2E_3Q\right)/\left[2(Q + E_3\cos\chi - E_3)\right]. \tag{2.19}$$

Our (ε, δ) cut modifies this boundary as follows

$$\text{(i)} \quad \chi > \delta,$$

$$\text{(ii)} \quad E_1^{\min} = \varepsilon Q, \qquad E_1^{\max} = \frac{Q(1-2\varepsilon)}{2(1-2\varepsilon\xi)}. \tag{2.20}$$

The cut on $E_1^{\max}$ simply reflects that $E_3^{\min} = \varepsilon Q$. Thus, a cut on (ε, δ) is simply a cut on the allowed physical phase space for a given process. The other cases involving the pairs "23" and "12" can be treated likewise.

With the definitions (2.16)–(2.20) it is a straightforward matter to calculate the EEC function $F(\xi, \varepsilon)$ from eq. (2.1). Recalling the definition of $F(\xi, \varepsilon)$ from our introduction

$$\frac{1}{\sigma_0}\frac{\mathrm{d}\Sigma^{\mathrm{c}}(\varepsilon, \delta)}{\mathrm{d}\cos\chi} = \frac{\alpha_s(Q^2)}{\pi} F(\xi, \varepsilon), \qquad \delta < \chi < 180^\circ - \delta,$$

we quote the result for $F(\xi, \varepsilon)$

$$F(\xi, \varepsilon) = \frac{1}{6\xi^5(1-\xi)}\Bigg[3(1-\varepsilon\xi)^2(2\xi-1) + 6(1-\varepsilon\xi)(4\xi^2-9\xi+4) + \frac{3}{1-\varepsilon\xi} \times \left\{\frac{(1-\xi)^2(1-2\xi)}{1-\varepsilon\xi} - 2(1-\xi)(4\xi^2-9\xi+4)\right\} + 2\ln\big((1-\varepsilon\xi)^2/(1-\xi)\big)(4\xi^3-18\xi^2+24\xi-9)\Bigg]. \tag{2.21}$$

Note that the leading-log behaviour is independent of ε and in the limit $\varepsilon \to 0$ one recovers

$$\lim_{\varepsilon \to 0} F(\xi, \varepsilon) = F(\xi),$$

where $F(\xi)$ is the $O(\alpha_s)$ BBEL function. It is worthwhile to do an expansion of the function $F(\xi, \varepsilon)$ in ε. Keeping up to $O(\varepsilon)^2$ terms we find the result already given in eq. (1.13),

$$F(\xi, \varepsilon) = F(\xi) - \tfrac{2}{3}\varepsilon\frac{1}{\xi(1-\xi)} + \frac{\varepsilon^2(3-2\xi)}{6\xi(1-\xi)} + O(\varepsilon)^3.$$

Thus, as remarked earlier the effect of imposing a cut on ε results in a power correction which starts at order $\varepsilon = \min E_i/\sqrt{s}$. Not surprisingly perturbative power corrections to the EEC function have a $1/Q$ dependence, just as in the Sterman-Weinberg 3-jet cross section to the same order.

However, as we have remarked earlier, the asymmetric EEC function $A(\xi, \varepsilon)$ defined in eq. (1.14) receives contribution to order $\varepsilon^2 = \min E_i^2/s$. Restating the result in eq. (1.15) we have

$$A(\xi, \varepsilon) = A(\xi) + \frac{\varepsilon^2(2\xi - 1)}{3\xi(1-\xi)} + O(\varepsilon^3).$$

Thus, at least in the perturbation theory, *power corrections to* $d\Sigma^A/d\cos\chi$ *fall off as* $1/Q^2$. This is in contrast to most other known jet measures and puts the asymmetric cross section on a somewhat higher pedestal among a host of perturbative jet measures, most of which have power corrections falling off like $1/Q$. Certainly the total hadronic cross section is better behaved, with power corrections to the unit operator $\langle I \rangle$ falling off like $1/Q^4$. However, as is well-known the leading coefficient in σ is independent of $\alpha_s(Q^2)$, whereas in $d\Sigma^A/d\cos\chi$ it is proportional to $\alpha_s(Q^2)$.

In table 3 we present the numerical results for $F(\xi, \varepsilon)$ for $\varepsilon = 0.05$, 0.10 and 0.15 for the angular range $0.05 \leqslant \xi \leqslant 0.95$. The result for $F(\xi, \varepsilon = 0.1)$ is compared with the BBEL function $F(\xi)$ in fig. 2. The large dependence of $F(\xi, \varepsilon)$ on ε is rather uncomfortable. Based on this perturbative result we *do* expect that non-perturbative power corrections to the BBEL function should also be large and this is in qualitative agreement with the observations by experimental groups and our previous analysis [3].

TABLE 3
The $O(\alpha_s)$ EEC function $F(\xi, \varepsilon)$ with $\varepsilon = 0.05, 0.1, 0.15$ and $\delta = 26°$

cos χ	ε = 0.05	ε = 0.10	ε = 0.15
−0.90, −0.80	7.782	6.852	5.938
−0.80, −0.70	3.865	3.296	2.745
−0.70, −0.60	2.576	2.102	1.698
−0.60, −0.50	1.381	1.535	1.208
−0.50, −0.40	1.515	1.216	0.937
−0.40, −0.30	1.289	1.019	0.770
−0.30, −0.20	1.141	0.891	0.662
−0.20, −0.10	1.043	0.806	0.590
−0.10, 0.00	0.981	0.750	0.541
0.00, 0.10	0.945	0.716	0.510
0.10, 0.20	0.933	0.702	0.493
0.20, 0.30	0.945	0.705	0.490
0.30, 0.40	0.983	0.778	0.500
0.40, 0.50	1.055	0.776	0.527
0.50, 0.60	1.180	0.862	0.580
0.60, 0.70	1.398	1.016	0.675
0.70, 0.80	1.819	1.314	0.865
0.80, 0.90	2.878	2.067	1.346

TABLE 4
The $O(\alpha_s)$ asymmetric EEC function $A(\xi, \varepsilon)$ with $\varepsilon = 0.05, 0.1, 0.15$, and $\delta = 26°$

$\cos\chi$	$\varepsilon = 0.05$	$\varepsilon = 0.10$	$\varepsilon = 0.15$
0.90, 0.80	4.904	4.785	4.591
0.80, 0.70	2.046	1.982	1.880
0.70, 0.60	1.128	1.086	1.022
0.60, 0.50	0.701	0.672	0.628
0.50, 0.40	0.460	0.440	0.409
0.40, 0.30	0.306	0.291	0.270
0.30, 0.20	0.195	0.186	0.172
0.20, 0.10	0.109	0.104	0.096
0.10, 0.00	0.035	0.033	0.031

In table 4 we present the results for the asymmetric EEC function $A(\xi, \varepsilon)$ for the same values of ε and δ as in table 3. The result $A(\xi, \varepsilon = 0.1)$ is compared with the BBEL function in fig. 3. Note the relative insensitivity of $A(\xi, \varepsilon)$ to ε. This is indeed satisfying and *we expect that the non-perturbative power corrections should likewise be small.* This feature is also strongly suggested by the data.

So much for the power corrections in the $O(\alpha_s)$ EEC cross section. Next we calculate the effect of the (ε, δ) resolution in order α_s^2 radiative corrections. First note that the preceding discussion in $O(\alpha_s)$ applies as such for the virtual EEC cross section given by eq. (2.8) and appendix A. One again uses the transformations and cuts defined through eq. (2.16)–(2.22). Again, the resulting expression involves a one-dimensional integral, the limits of which take into account the ε-cuts and the δ-cut is defined as before via eq. (2.16). Again, this contribution can be evaluated with arbitrary precision.

Let us now concentrate on the real 4-parton contribution. Since one is now bound to combine soft-partons, the results are specific to the prescription that one is using. We define below our recombination procedure.

If the partons in an event satisfy the ε-cut, then the δ-cut is imposed as in the 3-parton case using the definition (2.16). If, however, $\min(E_i/\sqrt{s}) < \varepsilon$, then the four-momenta of the partons having the smallest invariant mass are combined. The EEC for the resulting equivalent 3-parton state is calculated exactly as described before for the $O(\alpha_s)$ case. Alternatively, one could have checked that if two of the partons have energies less than $\varepsilon\sqrt{s}$, then the event could be classified as a 2-parton event and not included in the calculation of $d\Sigma^c$ at all. However, so long as $\varepsilon \ll 1$, the difference in the two prescriptions is small and we shall neglect it in further discussions*.

* There is yet another prescription of combining partons, e g the FSSK scheme [12] They define an "average" Sterman-Weinberg cross section by averaging the energy of the soft parton However, the difference between this scheme and any other would lie in $O(\varepsilon, \delta)$ and $O(y^{1/2})$ terms which they have neglected in, for example, the calculation of $d\sigma/dx_{max}$

We present our results for the (ε, δ)-dependent EEC cross section analogous to the case with no resolution dependence

$$\frac{1}{\sigma_0}\frac{\mathrm{d}\Sigma^{\mathrm{c}}(\varepsilon,\delta)}{\mathrm{d}\cos\chi} = \frac{\alpha_s(Q^2)}{\pi}F(\xi,\varepsilon) + \left(\frac{\alpha_s(Q^2)}{\pi}\right)^2 G(\xi,\varepsilon), \qquad \delta < \chi < 180^\circ - \delta,$$

$$\frac{1}{\sigma_0}\frac{\mathrm{d}\Sigma^{A}(\varepsilon,\delta)}{\mathrm{d}\cos\chi} = \left[\frac{\alpha_s(Q^2)}{\pi}A(\xi,\varepsilon) + \left(\frac{\alpha_s(Q^2)}{\pi}\right)^2 B(\xi,\varepsilon)\right]\theta(\chi-\delta). \tag{2.22}$$

The functions $R^{\mathrm{corr}}(\varepsilon,\xi)$ and $R^{\mathrm{asym}}(\varepsilon,\xi)$ have obvious definitions. The function $G(\xi,\varepsilon)$ is given in table 5 for $\varepsilon = 0.05$, 0.1 and 0.15 together with the fit values using the parametrization (2.12) for $R^{\mathrm{corr}}(\xi,\varepsilon)$. The values of the coefficients for the fit are given in table 6. The values of $R^{\mathrm{corr}}(\xi,\varepsilon)$ themselves are given in table 2. The fitted values of the $\mathrm{O}(\alpha_s)^2$ asymmetric EEC functions $B(\xi,\varepsilon)$ are put in table 7. In figs. 2 and 3 we plot the fitted function $G(\xi,\varepsilon)$ and $B(\xi,\varepsilon)$, respectively for $\varepsilon = 0$ and 0.1.

We would now like to discuss these results. Note that the dependence of $G(\xi,\varepsilon)$ on ε is very similar to that of the $\mathrm{O}(\alpha_s)$ BBEL function $F(\xi,\varepsilon)$. Both of them have power corrections starting in order ε. So qualitatively one could write

$$\frac{\mathrm{d}\Sigma^{\mathrm{c}}}{\mathrm{d}\cos\chi} = \frac{\alpha_s(Q^2)}{\pi}\left(F(\xi)+\mathrm{O}(\varepsilon)\right) + \left(\frac{\alpha_s(Q^2)}{\pi}\right)^2\left(G(\xi)+\mathrm{O}(\varepsilon)\right). \tag{2.23}$$

On the other hand, we see that the dependence of the $\mathrm{O}(\alpha_s)^2$ asymmetric function $B(\xi,\varepsilon)$ is also of order ε. Thus, one now has

$$\frac{\mathrm{d}\Sigma^{A}}{\mathrm{d}\cos\chi} = \frac{\alpha_s(Q^2)}{\pi}\left(A(\xi)+\mathrm{O}(\varepsilon)^2\right) + \left(\frac{\alpha_s(Q^2)}{\pi}\right)^2\left(B(\xi)+\mathrm{O}(\varepsilon)\right). \tag{2.24}$$

Amusingly, the perturbative power corrections to the asymmetric EEC functions $A(\xi)$ and $B(\xi)$ go in opposite directions. This is easy to understand since the effect of resolution on an initial 3-parton state is to promote it to a 2-parton state, thereby reducing the asymmetry. The effect of combining the 4-partons with (ε,δ) resolution works the opposite way, since a 4-parton state is in most cases more symmetric than a 3-parton state. The result is that the asymmetric EEC cross section calculated to $\mathrm{O}(\alpha_s)^2$ has still small power corrections, which is mainly due to the fact that $(\alpha_s/\pi)R^{\mathrm{asym}}(\xi)$ is itself a small number ~ 0.1 compared to 1. The effect of the (ε,δ) resolution on the asymmetric EEC cross sections is shown in fig. 4. We remark that the perturbative power corrections to the asymmetric EEC die out much faster in Q than in the correlation function itself or in the Sterman-Weinberg cross sections. This, very probably, is one of the reasons of good agreement between perturbation theory and the experimental data in this quantity.

TABLE 5
The $O(\alpha_s)^2$ EEC function $G(\xi, \varepsilon)$ with the same cuts as in table 3 (for each ε, the fitted values are also given)

$\cos\chi$	$\varepsilon = 0.05$		$\varepsilon = 0.10$		$\varepsilon = 0.15$	
−0.90, −0.80	76.65 ± 1.74	76.53	62.32 ± 1.78	62.00	45.59 ± 1.73	41.19
−0.80, −0.70	43.98 ± 1.74	37.49	33.83 ± 1.19	30.46	24.82 ± 1.16	22.92
−0.70, −0.60	24.34 ± 0.85	24.47	19.74 ± 0.88	19.78	14.53 ± 0.35	15.52
−0.60, −0.50	18.12 ± 0.79	18.39	14.00 ± 0.76	14.74	10.73 ± 0.72	11.69
−0.50, −0.40	14.87 ± 0.36	15.07	11.43 ± 0.83	11.97	5.42 ± 0.80	9.43
−0.40, −0.30	13.15 ± 0.55	13.11	10.56 ± 0.50	10.30	7.87 ± 0.48	8.00
−0.30, −0.20	12.69 ± 0.70	11.93	9.92 ± 0.69	9.27	7.19 ± 0.64	7.05
−0.20, −0.10	11.05 ± 0.07	11.24	5.31 ± 0.59	8.64	6.65 ± 0.35	6.41
−0.10, 0.00	11.51 ± 0.37	10.91	3.57 ± 0.35	8.30	6.18 ± 0.78	5.99
0.00, 0.10	10.38 ± 0.31	10.99	7.38 ± 0.59	8.19	4.93 ± 0.56	5.74
0.10, 0.20	10.74 ± 0.40	11.12	8.54 ± 0.34	8.29	5.76 ± 0.27	5.63
0.20, 0.30	11.01 ± 0.40	11.66	8.49 ± 0.32	8.60	6.15 ± 0.27	5.67
0.30, 0.40	12.61 ± 0.40	12.57	9.25 ± 0.40	9.18	6.17 ± 0.35	5.86
0.40, 0.50	13.77 ± 0.27	13.98	10.13 ± 0.53	10.12	6.48 ± 0.49	6.75
0.50, 0.60	16.39 ± 0.43	16.20	11.45 ± 0.41	11.62	6.97 ± 0.36	6.95
0.60, 0.70	21.24 ± 0.63	19.88	14.69 ± 0.56	14.13	8.42 ± 0.52	8.19
0.70, 0.80	27.74 ± 0.68	26.78	18.07 ± 0.59	18.87	9.41 ± 0.51	10.59
0.80, 0.90	42.84 ± 1.07	43.86	25.03 ± 1.00	30.63	10.83 ± 0.89	16.66

TABLE 6
The parameters in the fits for the function $R^{corr}(\xi, \varepsilon)$ with the χ^2/d.o.f

Coefficient ε	A	B	C	χ^2/d.o.f
0.0	3.01 ± 0.31	11.32 ± 0.21	−8.19 ± 0.9	23/15
0.05	4.90 ± 0.45	16.03 ± 0.29	−15.59 ± 1.14	14/15
0.10	4.06 ± 0.45	15.52 ± 0.38	−13.54 ± 1.44	9/14
0.15	0.64 ± 0.95	12.55 ± 0.55	−3.03 ± 2.53	22/13

TABLE 7
The $O(\alpha_s)^2$ functions for the asymmetric EEC $B(\xi, \varepsilon)$ with the same cuts as in table 3

$\cos\chi$	$\varepsilon = 0.05$	$\varepsilon = 0.10$	$\varepsilon = 0.15$
0.90, 0.80	32.661	31.372	24.532
0.80, 0.70	10.706	11.591	12.332
0.70, 0.60	4.587	5.650	7.335
0.60, 0.50	2.187	3.127	4.739
0.50, 0.40	1.088	1.849	3.180
0.40, 0.30	0.543	1.122	2.141
0.30, 0.20	0.263	0.668	1.383
0.20, 0.10	0.116	0.355	0.777
0.10, 0.00	0.032	0.111	0.251

2.3 INCLUDING THE QUARK MASSES

We study in this section the effect of including the quark masses on the EEC functions. We do this in the approximation of keeping the mass terms only for the Born diagrams for the processes (1.4) and (1.5). In other words the cancellation of divergences between the $O(\alpha_s)^2$ virtual 3-parton cross section and the soft 4-parton real cross sections are still being done in the limit $m_q \to 0$.

Again, we consider the $O(\alpha_s)$ EEC first. Our basic formula is eq. (2.1), where now the density $\tilde{T}$ is to be obtained from the process (1.4) keeping the quark masses in the calculation. The effect of heavy quark masses has been considered in the one-gluon radiation process by Ioffe [18], who derived the differential energy distribution for the heavy quarks. We have verified his calculations and merely quote the relevant result. For our purpose, the relevant quantity is $\tilde{T}$,

$$\tilde{T} = \sum_{i,j} \frac{2E_i E_j}{Q^2} T_H(y_{12}, y_{13}, y_{23})\, \delta(\chi - \theta_{ij}), \tag{2.25}$$

where now the heavy-quark density is given by

$$T_H(y_{12}, y_{13}, y_{23}) = \frac{z^2 + z'^2}{(1-z)(1-z')} - \frac{4m^2}{Q^2}\left(\frac{1}{1-z} + \frac{1}{1-z'}\right) - \frac{2m^2}{Q^2}\left(\frac{1}{(1-z)^2} + \frac{1}{(1-z')^2}\right) - \frac{4m^4}{Q^4}\left(\frac{1}{1-z} + \frac{1}{1-z'}\right)^2, \tag{2.26}$$

where

$$z = 1 - \frac{m^2}{Q^2} - y_{23},$$

$$z' = 1 - \frac{m^2}{Q^2} - y_{13}. \tag{2.27}$$

It is straightforward to check that

$$\lim_{m \to 0} T_H(y_{12}, y_{13}, y_{23}) = T(y_{12}, y_{13}, y_{23}),$$

where $T(y_{12}, y_{13}, y_{23})$ is given in eq. (2.2). We present the result in the form of a double-differential distribution, the EEC function can then be obtained by calculating the one-dimensional integral. In analogy to (2.5) we now have

$$\frac{1}{\sigma_0}\frac{d^2\Sigma^c}{dz\, d\cos\chi} = \frac{1}{8}\frac{\alpha_s(Q^2)}{\pi} C_F[g_{12}(z,\chi) + 2g_{13}(z,\chi)] T_H, \tag{2.28}$$

where

$$g_{12} = 2\int \mathrm{d}z'\, z^2 z'^2 v_1 v_2\, \delta\big(1 - z + 2m^2/Q^2 - z'\big(1 - \tfrac{1}{2}z + \tfrac{1}{2}z v_1 v_2 \cos\chi\big)\big),$$

$$g_{13} = 2z^2 v_1 \frac{(2 - z - z'')^3}{1 - z},$$

$$z'' = 2 - z - \frac{2(1 - z)}{2 - z(1 - v_1 \cos\chi)},$$

$$v_1 = \big(1 - 4m^2/Q^2 z^2\big)^{1/2},$$

$$v_2 = \big(1 - 4m^2/Q^2 z'^2\big)^{1/2},$$

$$z = 2E_1/Q, \qquad z' = 2E_2/Q. \tag{2.29}$$

It is again a useful check to obtain eq. (2.3) from (2.28) in the limit $m \to 0$. We have done the z integration numerically due to the presence of velocity factors which render the analytic integration rather intractable*. Expressing the $O(\alpha_s)$ result as before

$$\frac{1}{\sigma_0}\frac{\mathrm{d}\Sigma(\xi, m)}{\mathrm{d}\cos\chi} = \frac{\alpha_s(Q^2)}{\pi} F(\xi, m), \tag{2.30}$$

we have tabulated the results for $F(\xi, m)$ in table 8 for $\sqrt{s} = 34$ GeV, where most of the PETRA data is concentrated. Again, it is a straightforward matter to evaluate the effect of the ε-cut. The results corresponding to the values $\varepsilon = 0$, 0.05, 0.1 and 0.15 for the ratio $F(\xi, m, \varepsilon)/F(\xi, \varepsilon)$ are given in table 8. Note that we have used $m_c = 1.8$ GeV, $m_b = 5.0$ GeV and neglected the quark masses for the u, d and s quarks.

It is clear that the quark mass effects in the EEC correlations are not entirely negligible even at $\sqrt{s} = 34$ GeV. The ratio $F(\xi, m, \varepsilon = 0)/F(\xi, \varepsilon = 0)$, for example, varies from 0.91 for $\xi = 0.925$ to about 0.84 for $\xi = 0.0725$. Thus, both the EEC function $F(\xi)$ and the asymmetric part $A(\xi)$ have quark mass corrections which are only decreasing as m/E_{beam}. This has a perceptible effect on the determination of the QCD scale parameter as we shall see in sect. 4.

Finally, we have used the massive-quark calculation for the process (1.5) reported in ref. [14]. This is also part of the Monte Carlo program, generally referred to as the

* Alternatively one could calculate the EEC with masses from the Ali et al. Monte Carlo [19], where mass terms for both the processes (1.4) and (1.5) are taken into account. However, we have used eq. (2.28) to check the accuracy of the Monte Carlo and the agreement is good.

TABLE 8
The ratio $F(\varepsilon, m)/F(\varepsilon)$ at $\sqrt{s} = 34$ GeV for $\varepsilon = 0, 0\,05, 0\,1$ and $0\,15$ and $\delta = 26°$

cos χ	$F(\varepsilon, m)/F(\varepsilon)$ at $\sqrt{s} = 34$ cm			
	$\varepsilon = 0\,0$	$\varepsilon = 0\,05$	$\varepsilon = 0\,10$	$\varepsilon = 0\,15$
−0 90, −0 80	0 9088 ± 0 0035	0 9201 ± 0 0034	0 9294 ± 0 0034	0 9397 ± 0 0034
−0 80, −0 70	0 9281 ± 0 0042	0 9433 ± 0 0041	0 9550 ± 0 0041	0 9576 ± 0 0041
−0 70, −0 60	0 9313 ± 0 0047	0 9493 ± 0 0047	0 9607 ± 0 0046	0 9671 ± 0 0046
−0 60, −0 50	0 9387 ± 0 0051	0 9546 ± 0 0051	0 9627 ± 0 0050	0 9693 ± 0 0051
−0 50, −0 40	0 9284 ± 0 0054	0 9461 ± 0 0054	0 9518 ± 0 0053	0 9642 ± 0 0054
−0 40, −0 30	0 9348 ± 0 0057	0 9494 ± 0 0057	0 9583 ± 0 0058	0 9659 ± 0 0059
−0 30, −0 20	0 9352 ± 0 0060	0 9501 ± 0 0059	0 9552 ± 0 0003	0 9608 ± 0 0064
−0 20, −0 10	0 9294 ± 0 0063	0 9469 ± 0 0065	0 9597 ± 0 0066	0 9717 ± 0 0071
−0 10, 0 00	0 9408 ± 0 0065	0 9566 ± 0 0066	0 9677 ± 0 0071	0 9767 ± 0 0074
0 00, 0 10	0 9290 ± 0 0066	0 9424 ± 0 0068	0 9554 ± 0 0074	0 9642 ± 0 0078
0 10, 0 20	0 9240 ± 0 0068	0 9388 ± 0 0071	0 9366 ± 0 0075	0 9479 ± 0 0085
0 20, 0 30	0 9311 ± 0 0070	0 9481 ± 0 0074	0 9581 ± 0 0079	0 9715 ± 0 0087
0 30, 0 40	0 9197 ± 0 0071	0 9398 ± 0 0077	0 9493 ± 0 0081	0 9457 ± 0 0090
0 40, 0 50	0 9218 ± 0 0073	0 9356 ± 0 0078	0 9359 ± 0 0084	0 9425 ± 0 0096
0 50, 0 60	0 9021 ± 0 0073	0 9227 ± 0 0090	0 9418 ± 0 0088	0 9372 ± 0 0098
0 60, 0 70	0 8850 ± 0 0074	0 9012 ± 0 0079	0 9124 ± 0 0088	0 9139 ± 0 0103
0 70, 0 80	0 8680 ± 0 0075	0 8839 ± 0 0081	0 8880 ± 0 0089	0 9001 ± 0 0106
0 80, 0 90	0 8438 ± 0 0076	0 8540 ± 0 0082	0 9609 ± 0 0091	0 8786 ± 0 0110

Ali et al. Monte Carlo [19]. We find that within our calculational precision (±4% on the $O(\alpha_s)^2$ EEC function $G(\xi, \varepsilon)$) the ratio $G(\xi, m, \varepsilon)/G(\xi, \varepsilon)$ is very close to the one for $F(\xi, m, \varepsilon)/F(\xi, \varepsilon)$, i.e. both the functions $F(\xi, m, \varepsilon)$ and $G(\xi, m, \varepsilon)$ have similar though not identical linear dependence on ε and $m/\sqrt{s}$. So, to a very good approximation, $R^{\text{corr}}(\xi, m, \varepsilon)$ is independent of $m/\sqrt{s}$*. Thus,

$$\frac{1}{\sigma}\frac{d\Sigma}{d\cos\chi}(\varepsilon, m) = \frac{\alpha_s}{\pi}F(\xi, m, \varepsilon)\left[1 + \frac{\alpha_s}{\pi}R^{\text{corr}}(\xi, \varepsilon)\right] + O(\varepsilon m/Q) + O(m^2/Q^2), \tag{2.31}$$

where $R^{\text{corr}}(\xi, \varepsilon)$ is the function with $m = 0$ (i.e the entries in table 2). The function $A(\varepsilon, m)$ and $R^{\text{asym}}(\xi, m, \varepsilon)$ can be obtained from $F(m, \varepsilon)$ (table 8) and $R^{\text{corr}}(\xi, \varepsilon)$ (table 2).

Let us briefly summarise the results of this section before we move on to the discussion of the non-perturbative effects in the EEC cross section.

(i) The $O(\alpha_s)^2$ corrections in the theoretical limit ($\varepsilon = \delta = 0$) are substantial for the EEC function $F(\xi)$. Typical corrections are $(7 - 10)\alpha_s/\pi$, and so the second-order corrections to $F(\xi)$ can be as large as ~ 40% at $\sqrt{s} = 30$ GeV.

* It is very likely that $R^{\text{corr}}(\xi, m)/R^{\text{corr}}(\xi)$ has $O(m^2/Q^2)$ corrections, but we neglect such higher-order terms here Again one could use the Ali et al Monte Carlo [19] to exactly take them into account

(ii) The order α_s^2 correction (in the limit $\varepsilon = \delta = 0$)) to the asymmetric EEC function $A(\xi)$ are small. Typical corrections are $\sim 3\alpha_s/\pi$ and so the second-order corrections to $A(\xi)$ can be as large as $\sim 15\%$ at $\sqrt{s} = 30$ GeV.

(iii) Imposing experimental resolution in the spirit of Sterman-Weinberg, we find the following behaviour

$$F(\varepsilon) = F(\varepsilon = 0)(1 + O(\varepsilon) + - - -),$$

$$G(\varepsilon) = G(\varepsilon = 0)(1 + O(\varepsilon) + - - -),$$

$$A(\varepsilon) = A(\varepsilon = 0)\big(1 + O(\varepsilon)^2 + - - -\big),$$

$$B(\varepsilon) = B(\varepsilon = 0)(1 + O(\varepsilon) + - - -), \tag{2.34}$$

which leads us to conclude that at least in the perturbation theory power corrections to $d\Sigma^A$ are small.

(iv) Quark mass corrections to all the functions $F(\xi)$, $G(\xi)$, $A(\xi)$ and $B(\xi)$ are linear in $m/\sqrt{s}$. The effect at $\sqrt{s} = 34$ GeV is typically about 10%. Thus, it is important to keep them for a quantitative determination of the scale parameter Λ

3. Non-perturbative contribution to the EEC

In this section we evaluate the non-perturbative fragmentation contribution to the EEC cross section. Needless to say that in the absence of a complete theory of confinement this is bound to be model dependent. Before we embark upon a detailed model of the quark and gluon fragmentation, we would like to discuss some aspects of fragmentation that are quite general and deserve consideration.

The first point concerns the effect of longitudinal momentum distribution. It can be easily proven that the EEC, in the first approximation, is independent of the details of how quarks and gluons fragment their longitudinal momentum, so long as the fragmentation products are almost *collinear* with the parent parton. This is simply a consequence of energy-momentum conservation. Thus, the longitudinal fragmentation functions in the first approximation can be neglected. Perhaps, it is worthwhile to remark that this property is specific to the EEC only. If higher powers of the energy are used as weight factors, then the information on the single-particle inclusive distribution (i.e. longitudinal momentum fragmentation functions) is *essential* to determine the normalization. Consequently, higher moments are more model dependent.

Thus, the single most important feature for the EEC is the p_T profile of a quark and gluon jet. However, it is now generally appreciated that only limited-p_T fragmentation models can explain the appearance of jets in e^+e^- annihilation and elsewhere. Let us then take, for the sake of argument, the limited-p_T model of Field

and Feynman [20] which has the following hadronic-p_T distribution

$$f(p_T^2) = \frac{1}{2\sigma_q^2} e^{-p_T^2/2\sigma_q^2}, \tag{3.1}$$

where σ_q is a free parameter and has to be determined from the p_T distribution of hadrons. (We stress here that the detailed features of the Field-Feynman model are not relevant for our qualitative arguments.) It is worthwhile to look at the EEC in the central region (i.e. near $\chi \simeq 90°$). Now by definition $\sin\chi = p_T/p_L$. However, since p_T is cut off due to (3.1) but p_L is almost scaling with energy (again a phenomenological fact) we see that $\sin\chi$ falls off like $\sim 1/\sqrt{s}$ with energy. Thus, in all limited-p_T models, the contribution to the EEC in the central region must fall off like $1/\sqrt{s}$ if only the process (1.3) (i.e. $e^+e^- \to q\bar{q}$) is considered. Also at a given c.m. energy the EEC itself should have an exponential behaviour approximately of the form

$$\frac{d\Sigma^c}{d\cos\chi} \sim e^{-\alpha|\sin\chi|}, \tag{3.2}$$

where α is a function of σ_q, and this again is a consequence of (3.1).

The behaviour (3.2) and the independence of EEC from the p_L distribution is a simplified picture and it is certainly going to change as more realistic features of heavy quark, resonance production and decays are taken into account. However, it is satisfying that a realistic model [20] incorporating these features still maintains the qualitative argument (3.2). This is shown in fig. 6, where we plot the contribution to the EEC from $q\bar{q} \to$ hadrons using the Field-Feynman model. Note the $1/\sqrt{s}$ dependence of $d\Sigma^c/d\cos\chi$ in the central region ($60° < \chi < 120°$) as $\sqrt{s}$ increases from 22 GeV to 60 GeV, and the almost exponential behaviour of eq. (3.2).

Another consequence of eq. (3.1) is that it predicts an exponential fall-off for the asymmetric EEC cross section $d\Sigma^A/d\cos\chi$ with *both* $\cos\chi$ and $\sqrt{s}$. Again the expectation of the Field-Feynman model is shown in fig. 7, where we show the cross section $d\Sigma^A/d\cos\chi$ for $\sqrt{s} = 22$, 34, 45 and 60 GeV. Also shown is the behaviour of the asymmetric correlation cross section at $\cos\chi = 0.925$, and it falls down exponentially with energy.

Thus going to sufficiently high energy, for example $\sqrt{s} \geqslant 20$ GeV, the $q\bar{q} \to$ hadron contribution to $d\Sigma^A/d\cos\chi$ becomes entirely negligible for $\chi \geqslant 30°$. So, if one is interested in a study of the QCD processes (1.4) and (1.5), the cross section $d\Sigma^A/d\cos\chi$ at $\sqrt{s} \geqslant 20$ GeV provides a kinematic domain in χ free of $q\bar{q} \to$ hadron contamination. Of course, all of this is well-known to our experimental colleagues.

Let us now turn to the fragmentation effects in the processes (1.4) and (1.5) involving at least one-gluon radiation. The difference with respect to the $q\bar{q}$ production is that now the perturbation theory itself provides a continuous distribu-

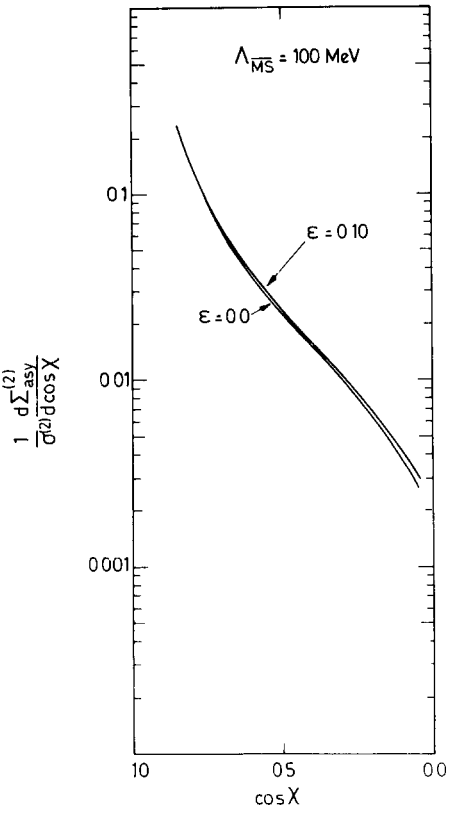

Fig 5 The cross section $d\Sigma^A/d\cos\chi$ in perturbative QCD calculated up to $O(\alpha_s)^2$ The solid line is the theoretical limit $\varepsilon = \delta = 0$, the dashed line corresponds to a cut $\varepsilon = 0\,1$, $\delta = 26°$ The curves are drawn for $\Lambda_{\overline{MS}} = 100$ MeV and $\sqrt{s} = 34$ GeV

tion for $d\Sigma^c/d\cos\chi$ and $d\Sigma^A/d\cos\chi$ at all angles [1]. Thus, it is not possible to separate the perturbative and non-perturbative components just kinematically. However, if the fragmentation of quarks and gluons involves a limited-p_T phenomenon, which is strongly suggested from the existence of 2, 3 and 4 jets in e^+e^- annihilation, then the additional contribution to $d\Sigma^c/d\cos\chi$ from the fragmentation should fall down like $1/\sqrt{s}$ with energy. This is exactly what happens in $d\Sigma^c/d\cos\chi$ from $q\bar{q} \to$ hadrons, as we have already shown. Thus, here also the most important parameter is the intrinsic p_T of the hadron. In fact, since the p_T distributions of hadrons from the quark and gluon jets are qualitatively very similar at PETRA energies, the non-perturbative contribution to the EEC is essentially *fixed* from inclusive p_T-distribution measurements.

Again, the correlation is itself more sensitive to the intrinsic p_T of hadrons but the asymmetry is relatively insensitive to its precise value (much in the spirit of the ε-dependence of the EEC functions $F(\varepsilon)$ and $A(\varepsilon)$).

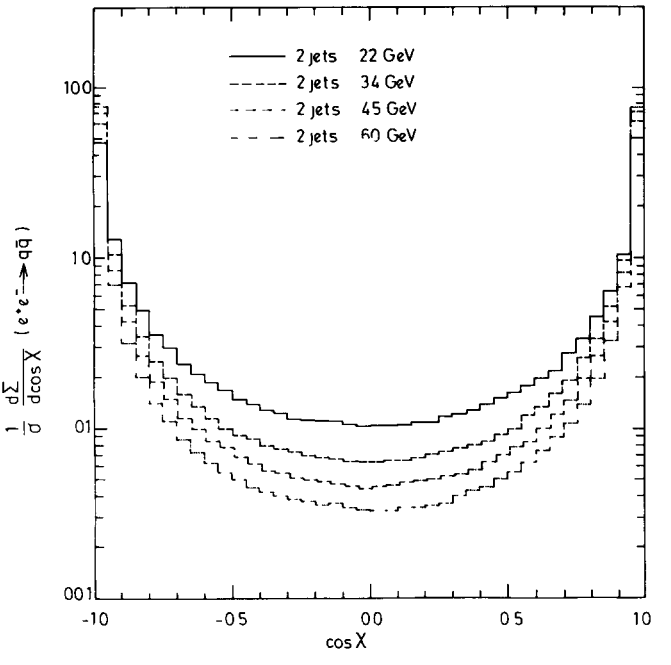

Fig 6 The EEC cross section $d\Sigma^c/d\cos\chi$ for the process $e^+e^- \to q\bar{q}$ using the model (21) for $\sqrt{s} = 22$, 34, 45 and 60 GeV

To give a quantitative content to these arguments we show in fig. 8 the predictions of a limited-p_T fragmentation model *without* any long-range colour correlations [19]. We see that such so-called independent-jet models (IJM) give rise to fragmentation components in $d\Sigma^A/d\cos\chi$ which are very close to the perturbation theory distributions The fit to $d\Sigma^A/d\cos\chi$ shown in fig. 8 corresponds to the function (for $\chi > 25°$)

$$\frac{1}{\sigma}\frac{d\Sigma^A_{\text{frag}}}{d\cos\chi}(\chi) \simeq \frac{\alpha_s(Q^2)}{\pi}\frac{1}{\sqrt{s}}C\left[A(\xi) + \frac{\alpha_s(Q^2)}{\pi}B(\xi)\right], \tag{3.3}$$

where C (GeV) $= -6.3 \pm 1.3$. The coefficient C does not depend sensitively on the p_T of the hadrons. This is shown in fig. 9, neither does it depend on the fragmentation function of the gluon, which is shown in fig. 10 where we have compared two realistic $G \to q\bar{q} \to$ hadrons functions. The first is the one due to Altarelli and Parisi [21]

$$f_G^q(z) = z^2 + (1-z)^2, \tag{3.4}$$

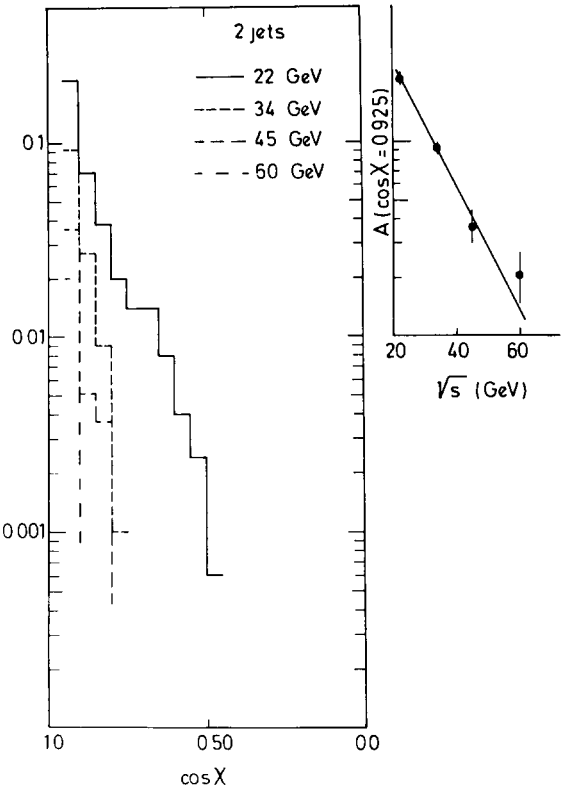

Fig 7 The EEC asymmetric cross section $d\Sigma^A/d\cos\chi$ from the process $e^+e^- \to q\bar{q}$ using the model (21) for $\sqrt{s} = 22$, 34, 45 and 60 GeV The outset is the $\sqrt{s}$ dependence of the distribution $d\Sigma^A/d\cos\chi$ for the bin $0\,9 \leqslant \cos\chi \leqslant 0\,95$

with

$$z = E_q/E_G,$$

and the other is a constant fragmentation function

$$f_G^q(z) = \text{const}. \tag{3.5}$$

The error in the coefficient C takes into account all such dependences. Thus, we emphasize again that the profile fof the fragmentation function in the EEC is not a freely moving contour but is tightly constrained, once the inclusive-p_T distribution is fixed by an independent measurement.

The relative importance of the non-perturbative effects in $d\Sigma^A/d\cos\chi$, typically at $\sqrt{s} = 30$ GeV, is of order 15% and decreases as $\sim 1/\sqrt{s}$ with energy. This is shown

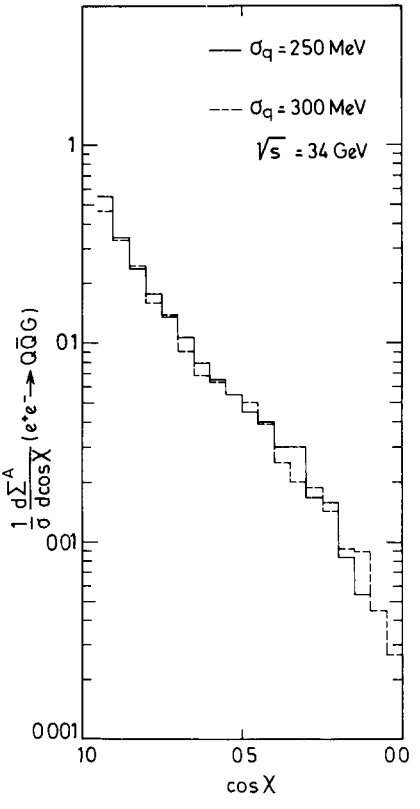

Fig 8 The dependence of the fragmentation component in $d\Sigma^A/d\cos\chi$ on the intrinsic p_T of the hadrons The solid line corresponds to $\sigma_q = 0\,25$ GeV and the broken line is for $\sigma_q = 0\,3$ GeV

in fig. 10. Thus, despite being complicated models with strong correlations among various input parameters, the independent jet models have a very definite prediction about the distribution $d\Sigma^A/d\cos\chi$ and its energy dependence. This is certainly testable at PETRA energies.

Before we close this section we would like to reiterate what was first realised by Ellis [22], and which was later confirmed by various independent experimental groups, that long-range colour correlations, as for example in the LUND model [23], lead to a quantitatively different non-perturbative estimate than is given in eq. (3.3) for the independent jet models. Based on $O(\alpha_s)$ considerations Ellis estimated [22]

$$\frac{d\Sigma^A_{\text{string frag}}(\chi)}{d\cos\chi} \simeq \frac{\alpha_s(Q^2)}{\pi}\frac{1}{\sqrt{s}} C_{\text{string}} A(\xi) \tag{3.6}$$

with

$$C_{\text{string}} = -16.6.$$

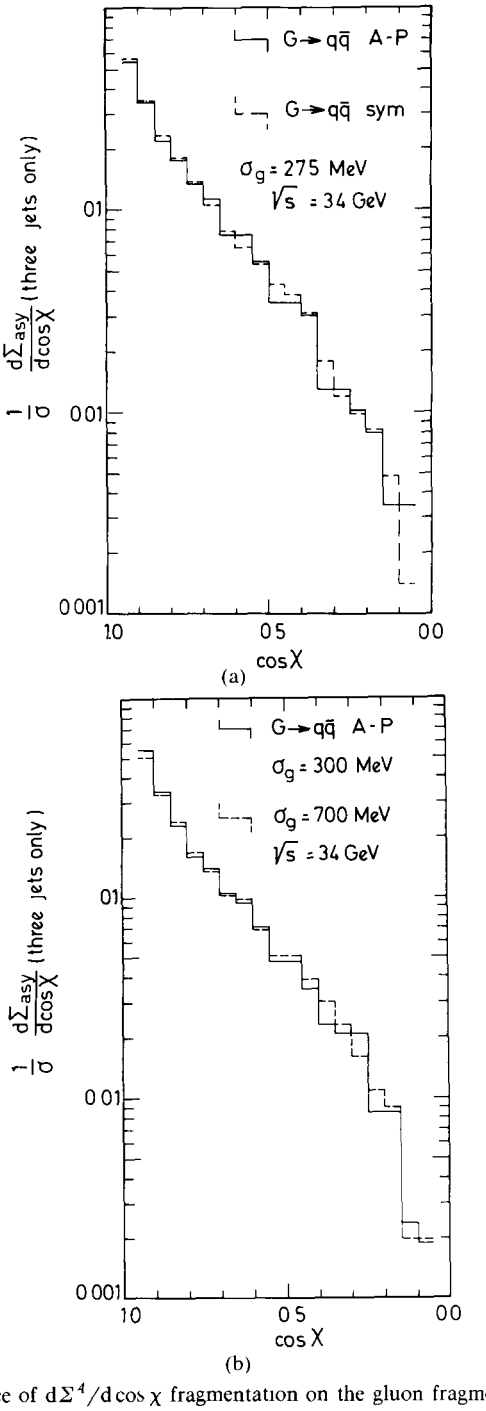

Fig 9 (a) The dependence of $d\Sigma^A/d\cos\chi$ fragmentation on the gluon fragmentation function $g \to q\bar{q} \to$ hadrons The solid line assumes the Altarelli-Parisi form for $g \to q\bar{q}$ and the broken line is for a constant $g \to q\bar{q}$ fragmentation function (b) The dependence of $d\Sigma^A/d\cos\chi$ on σ_g

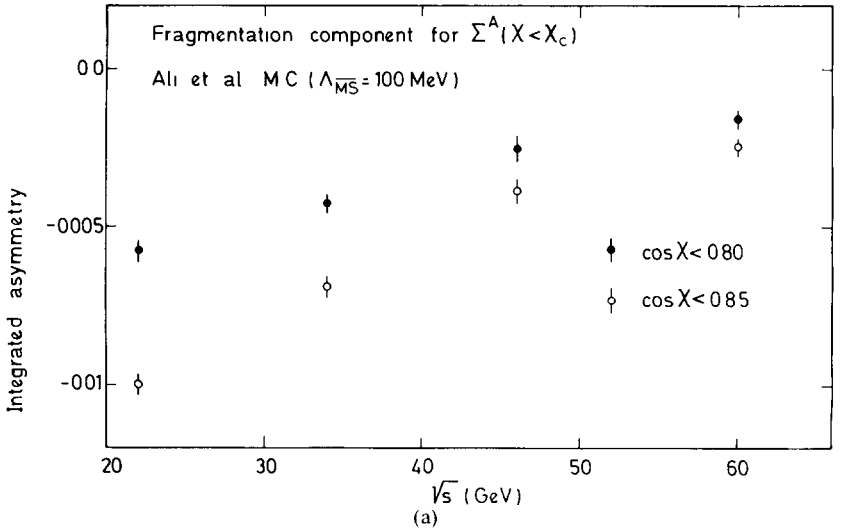

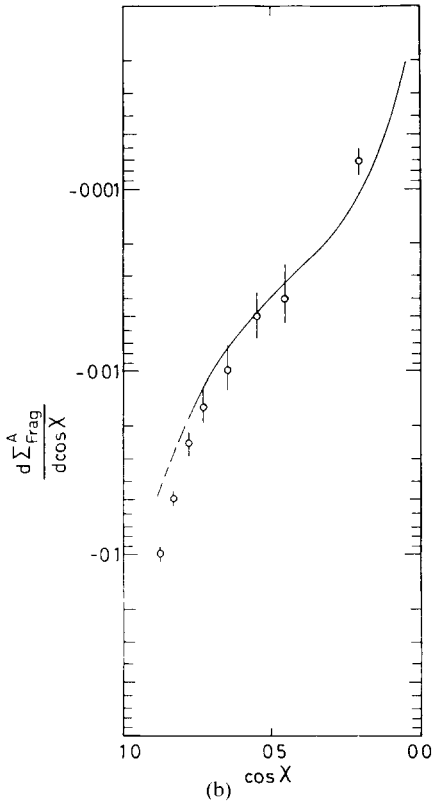

Fig 10 (a) The energy dependence of the integrated asymmetric cross section

$$\Sigma^A(\chi > \chi_c) = \frac{1}{\sigma}\int_{\chi>\chi_c} d\Sigma^A/d\cos\chi\, d\cos\chi$$

(only fragmentation component) from the Ali et al model [19] (b) The distribution $d\Sigma^A_{frag}/d\cos\chi$ (histogram) from the same model at $\sqrt{s} = 34$ GeV The solid line is the fit using (3 4) (c) Effect of (ε, δ) cuts on $d\Sigma^A/d\cos\chi$

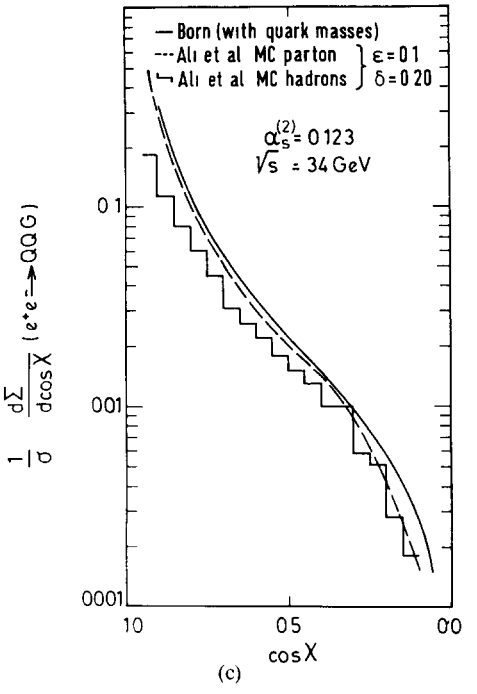

(c)

Fig 10 (continued)

Thus, the non-perturbative power corrections in the string model are *substantial* to the $O(\alpha_s)$ asymmetric EEC function $A(\xi)$. This is in contrast to the expectations of power corrections to $A(\xi)$ in perturbation theory. What happens if $O(\alpha_s)^2$ effects are also included and the fragmentation on the 4-parton states (1.5) are taken into account à la LUND string? The qualitative effect of the string induced correlation remains. Estimates vary from ~ 35% to ~ 70% about the relative contribution of non-perturbative effects in the LUND model if second-order terms are included in eq. (3.5). In any case, the non-perturbative contribution to $d\Sigma^A/d\cos\chi$ is discernably larger in models with strong colour correlations as opposed to the IJM estimates given in (3.3). This difference again is testable experimentally at PETRA and TRISTAN energies.

4. Comparison with experimental data

We would now like to make a comparison of the $O(\alpha_s)^2$ calculations reported in sect 2 with the data. This will be done both at the parton level (i.e. using only perturbation theory results) and including the hadronization effects as discussed in sect. 3. We recall that such a comparison was already made in ref. [3]. However, since our theoretical calculations for the function $B(\xi)$ have changed somewhat for

large χ, and we have included the quark mass and experimental resolution effects we repeat this comparison. Recently the Mark-J collaboration [5] have analysed their data using the calculations described in this paper and in ref. [19]; we will use their determination of $\alpha_s(Q^2)$ and compare it with the ones here. See also ref. [4] for similar phenomenological analysis

4 1 PERTURBATION THEORY VERSUS EEC DATA

We remark that testing the bare perturbation theory matrix element in "popular jet measures" like $\langle 1 - T \rangle$, $\langle \sin^2\delta \rangle$, the average heavy jet mass $\langle M_H/\sqrt{s} \rangle$ or the EEC itself is a formidable proposition at PETRA/PEP energies precisely because of the large power corrections. This can be seen in fig. 11, which we are including here to stress our point. The data come from the PLUTO collaboration [24]. The solid curves are the fits using a $\ln s + b/\sqrt{s}$. It is clear that the coefficient b/a, which is the measure of non-perturbative power corrections, is *not* small. In contrast, the asym-

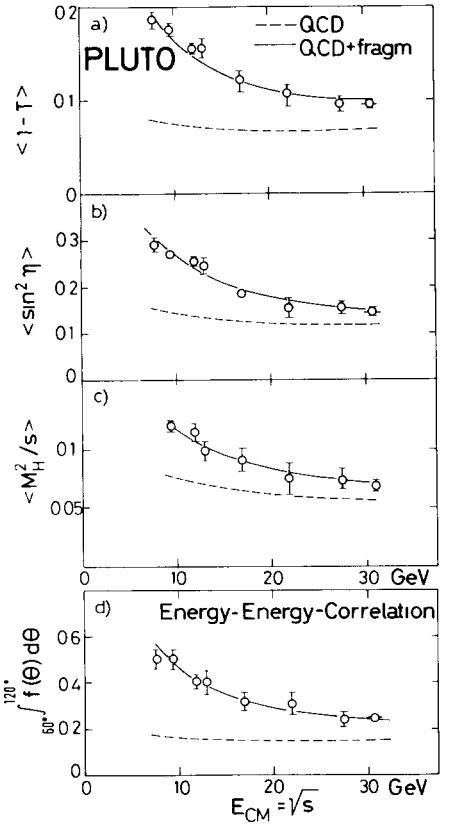

Fig 11 Energy dependence of some jet measures at PETRA energies The solid line is a fit $a \ln Q + b$ The dashed curve is the perturbative QCD prediction ($O(\alpha_s)$) The figure is taken from ref [24]

metric EEC cross section

$$\Sigma^A(\chi > 35°) \equiv \int_{\chi > 35°} \mathrm{d}\Sigma^A/\mathrm{d}\cos\chi\,\mathrm{d}\cos\chi$$

shown in fig. 12 indicates little (if any) energy dependence in the DORIS-PETRA energy region 9.4 GeV $\leqslant \sqrt{s} \leqslant$ 34 GeV. Though there are systematic errors involved and the statistics of the data shown are not very high, nevertheless a certain qualitative difference between the jet measures in figs. 11 and 12 is clearly visible.

Based on our prejudgement of power corrections in perturbation theory on the one hand, and the remarkable constancy of $\Sigma^A(\chi > 35°)$ on the other, we concentrate in this subsection on the asymmetric EEC at large angles.

In fig. 13 we show a comparison of the CELLO and PLUTO data [5,2] and compare the complete $O(\alpha_s)^2$ perturbative results *including* the quark mass terms. The shape of the $O(\alpha_s)^2$ perturbation theory distribution is in good agreement with the data for $\chi > 30°$. Thus, not only does the $\sqrt{s}$ dependence of $\Sigma^A(\chi)$ but also the differential distribution for $\chi > 30°$ hints that at least in the EEC we are already in the perturbative region. Fitting the tail of the distribution we find

$$\Lambda_{\overline{\mathrm{MS}}} = 132^{+101}_{-80}\ \mathrm{MeV}, \qquad \text{PLUTO},$$

$$= 160^{+64}_{-52}\ \mathrm{MeV}, \qquad \text{CELLO}.$$

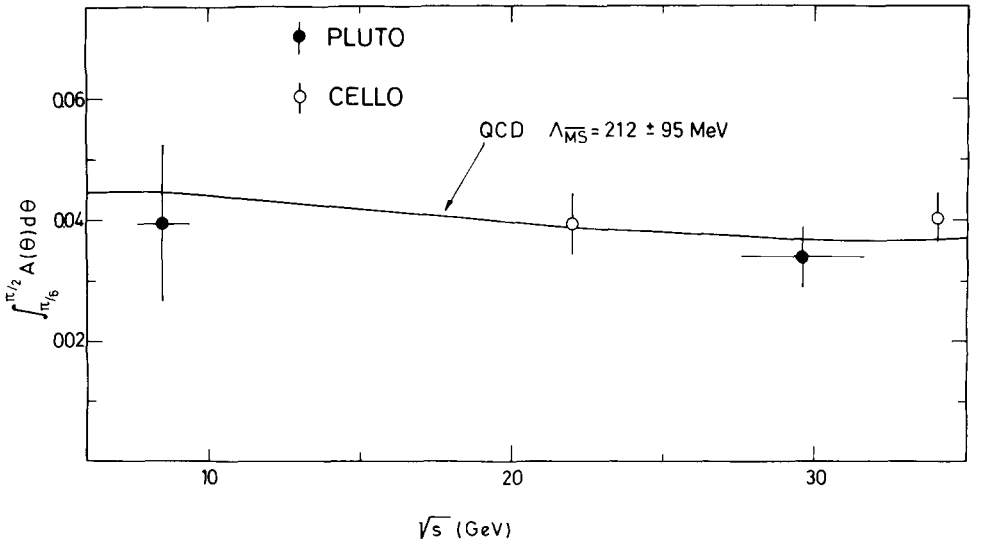

Fig 12 The integrated asymmetric cross section $\Sigma^A(\chi > 35°)$ from the PLUTO [2] and CELLO [5] collaborations in the range 9 4 GeV $\leqslant \sqrt{s} \leqslant$ 34 GeV The solid line is the fit using the complete $O(\alpha_s)^2$ calculations and the fragmentation component from eq (3 3)

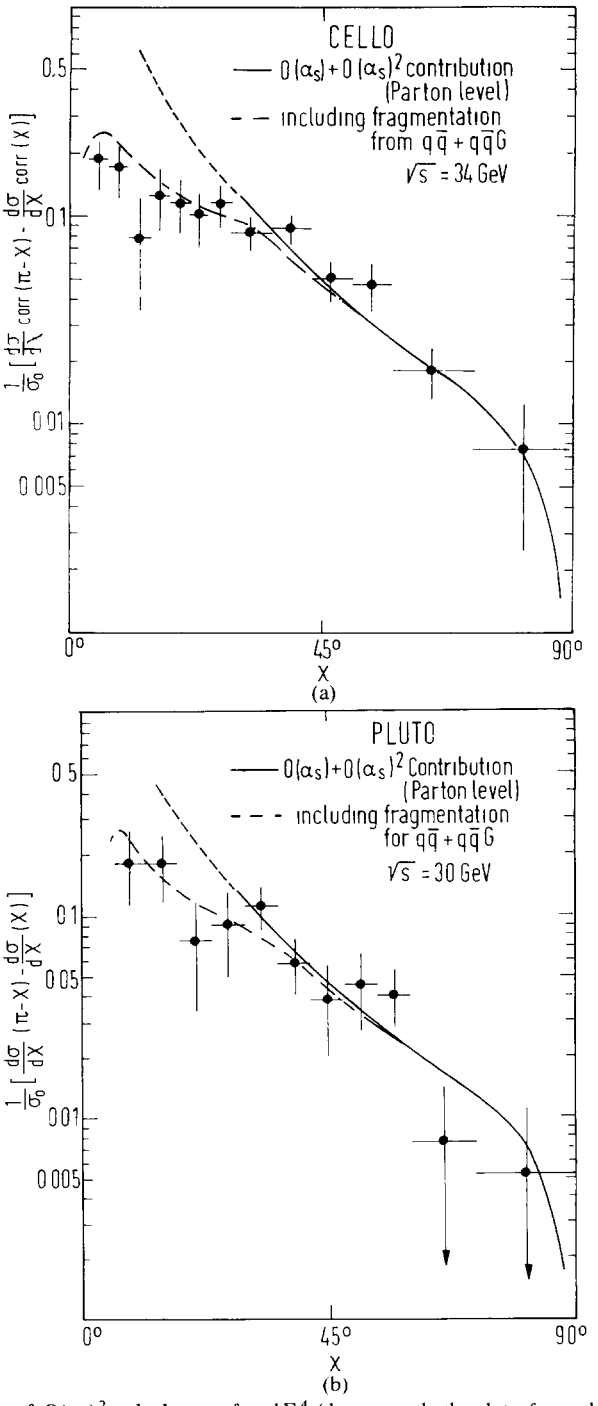

Fig 13 Comparison of $O(\alpha_s)^2$ calculations for $d\Sigma^4/d\cos\chi$ with the data from the PLUTO [2] and CELLO [5] collaboration The solid line includes the fragmentation effects using the Ali et al model [19], the broken line is the result of extrapolating the perturbation theory result to small angles At large angles, the two lines coincide for the different $\Lambda_{\overline{MS}}$ values quoted in the text

These numbers are slightly higher compared to the ones reported in ref. [3], mainly because of the inclusion of quark mass terms, but to some extent due to the change in the B function*. Thus, we determine that $\Lambda_{\overline{\rm MS}} = 146^{+60}_{-47}$ MeV. This is to be contrasted with the world average $\Lambda_{\overline{\rm MS}} = 160^{+100}_{-80}$ MeV, or from a recent analysis [25] of the $O(\alpha_s)^4$ calculations of the J/ψ and Υ widths, giving $\Lambda_{\overline{\rm MS}} = 136^{+62}_{-37}$ MeV from the J/ψ, and $\Lambda_{\overline{\rm MS}} = 133^{+46}_{-35}$ MeV from the Υ decays. The agreement is remarkable! Nevertheless, we should point out that the value of $\Lambda_{\overline{\rm MS}}$ so determined is a lower bound, since all non-perturbative power corrections have been ignored, which if the data is taken on its face-value are small. Thus, even modest statistical data in the asymmetric EEC cross section like the one used here provides a *non-trivial lower bound* on $\Lambda_{\overline{\rm MS}}$, namely at 68% CL $\Lambda_{\overline{\rm MS}} \geqslant 73$ MeV. This is a lower bound since all non-perturbative fragmentation contributions are negative (see sect. 3), which reduce the asymmetry, consequently requiring bigger $\alpha_s(Q^2)$ and hence $\Lambda_{\overline{\rm MS}}$**.

4.2 INCLUDING NON-PERTURBATIVE EFFECTS IN THE EEC

We now include the considerations of sect. 3 and evaluate the effect of fragmentation on the value of $\alpha_s(Q)$. As mentioned earlier we use the Ali et al. model [19] to implement quark, gluon fragmentation, and recall that in the $\chi > 30°$ asymmetric EEC cross section eq. (3.3) is a reasonable parametrization of this model for $\sqrt{s} \geqslant 20$ GeV.

Reanalysing the large-χ region now by including (3.2) with the $O(\alpha_s)^2$ perturbative calculations, we get again a reasonable fit of the data with the effect that $\alpha_s(Q^2)$ is now normalized upwards by ~ 10–15%. This is shown in fig. 13. We now obtain the following values

$$\Lambda_{\overline{\rm MS}} = 168^{+146}_{-103}\ \text{MeV}, \qquad \text{PLUTO},$$

$$= 278^{+64}_{-52}\ \text{MeV}, \qquad \text{CELLO},$$

$$= 140^{+40}_{-30}\ \text{MeV}, \qquad \text{MARK-J},$$

where we have used the published result of the MARK-J collaboration [5]. We average*** this value taking into account the statistical weight of the data and this

* The value of $\Lambda_{\overline{\rm MS}}$ at the parton level from the MARK-J data is very similar (private communication)

** The effect of the intrinsic p_T of the hadrons due to the fragmentation of quarks and gluons is to reduce the asymmetry from the $O(\alpha_s)$ process $e^+e^- \to q\bar{q}G$ Quark mass effects and weak decays of heavy quarks also reduce the asymmetry It is therefore very plausible that the non-perturbative effects to the perturbative QCD asymmetry are negative though we are not able to formulate this statement as a theorem

*** This averaging is legitimate since both we and the MARK-J collaboration use the $O(\alpha_s)^2$ calculations reported here and in refs [3,4], and the Ali et al model [19] to include the fragmentation effects

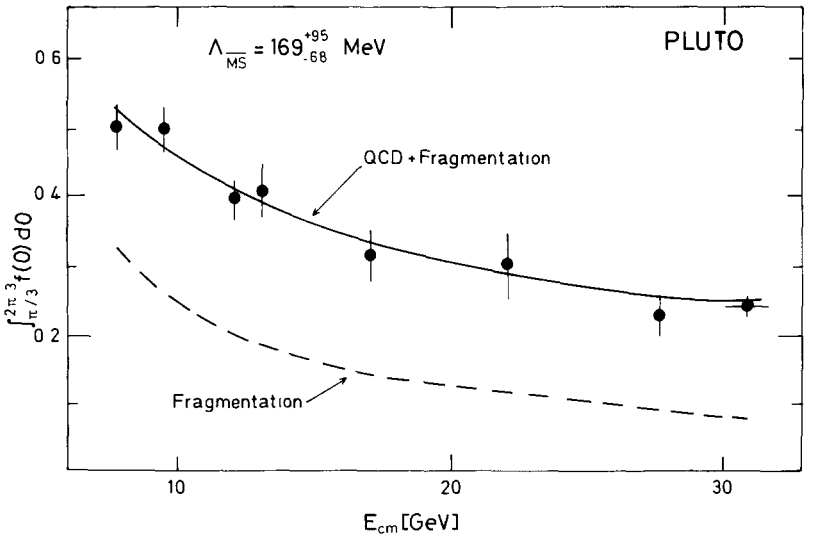

Fig 14 A comparison of the PLUTO data for the integrated correlation cross section $\Sigma^{corr}(\chi > \chi_c)$ in the range 9.4 GeV $\leqslant \sqrt{s} \leqslant$ 34 GeV with the Ali et al model [19] Also shown is the fragmentation component alone (broken line)

gives $\Lambda_{\overline{MS}} = 168^{+60}_{-40}$ MeV. Thus, $\alpha_s(Q^2 = 1225\ \text{GeV}^2) = 0.13 \pm 0.01$, which is consistent with the result from other determinations of $\alpha_s(Q^2)$ using, for example, the cluster algorithms and shape analysis; using similar models like the ones used here [27].

The value $\Lambda_{\overline{MS}} = 168^{+60}_{-40}$ MeV determined from the EEC asymmetry, is consistent with the EEC correlation cross section itself. This is shown in fig. 14 where a comparison is made with the integrated EEC cross section in the range 9.4 GeV $\leqslant \sqrt{s} \leqslant$ 33 GeV measured in the PLUTO collaboration. That the model in ref. (19) describes the EEC and the asymmetry for all measured angles χ is checked by the MARK-J collaboration and we refer to their papers [5] for detailed comparison.

We conclude this section by making a general remark that the value $\Lambda_{\overline{MS}} = 168^{+60}_{-40}$ MeV determined from the EEC asymmetry is an estimate specific to independent jet models, which *do not* take into account any long-range colour correlations. The form given in eq. (3.3) for $d\Sigma^A/d\cos\chi$ is a definite prediction and it should be a simple matter to check or rule out this dependence, once higher energies at PETRA, HERA e^+e^- or TRISTAN are available.

5. Summary and conclusion

The main motivation of the work reported in this paper was to understand theoretically the experimental result that the measured EEC asymmetric cross

section is remarkably energy independent in the entire PETRA/PEP range. The only other quantity showing this feature is the total hadronic cross section but there it is known that the power corrections fall off like $\sim 1/Q^4$ and hence they are not discernable in the PETRA/PEP data. The obvious interpretation of the EEC data is that the power corrections in the asymmetric cross section are likewise small. We demonstrated that this indeed is the case in perturbation theory where the leading asymmetric function $A(\xi)$ has power corrections, which fall off like $\sim 1/Q^2$.

We have no theoretical derivation of the non-perturbative power corrections but we argued that limited-p_T fragmentation models with *no* long-range colour correlations are very tightly constrained from the p_T distribution of hadrons. Given the p_T distribution experimentally, the fragmentation contribution to $d\Sigma^A/d\cos\chi$ is well determined. This component is also small in stringless models at PETRA energies and decreases as $1/Q$. Thus, the limited-p_T fragmentation models with *small* long-range colour correlations naturally explain the data. Unfortunately, the quality and close proximity (in energy) of the present data makes it difficult to check the $1/Q$ behaviour of eq. (3.3), but we do hope that such a test should be possible at the PETRA/PEP energies in the not-too-distant future.

We conclude by stating that the energy-energy correlation provides an excellent ground for perturbative QCD to confront data. At the same time it provides a rather definitive check of the power corrections in a way which is particularly sensitive to the presence or absence of long-range colour correlations.

We are grateful to our colleagues at DESY and Siegen for useful discussions. We particularly thank S. Brandt, G. Kramer, S.C.C. Ting, T. Walsh, R.Y. Zhu and members of the Mark-J collaboration for help, discussions and support. Finally we would like to acknowledge correspondence with S.D. Ellis and W.J. Stirling on the subject matter of this paper, and we thank them for sending us a copy of their paper prior to publication.

Appendix A

We write here the function $T_v(\omega, y)$ which appears in eq. (2.8) of the text for the virtual corrections to the EEC.

$$T_v(\omega, y) = T_{12}V_{12} + F_{12} + 2(T_{13}V_{13} + F_{13}). \tag{A.1}$$

The functions T_{12} and T_{13} are the same that occur in the order α_s calculations and are given in eqs. (2.4) of the text. The functions V_{12}, V_{13}, F_{12} and F_{13} are given below.

$$V_{12} = C_F\left[-\ln^2\frac{1-y}{y} - 2\ln\left(\frac{1-y}{y}\right)\ln\omega \right.$$
$$\left. -\ln^2 z - \tfrac{9}{2}\ln\frac{1-y}{y} - \tfrac{9}{2}\ln z - 2\,\mathrm{Li}_2(v/y) - 2\,\mathrm{Li}_2(1-z)\right]$$

$$+N_c\left[-\ln^2\left(\frac{1-y}{y}z\right)-\tfrac{11}{6}\ln z-2\,\mathrm{Li}_2(u/y)-\tfrac{11}{6}\ln\frac{1-y}{y}\right]$$

$$+T_R\left[\tfrac{2}{3}\ln\frac{1-y}{y}+\tfrac{2}{3}\ln z\right], \tag{A.2}$$

$$V_{13}=C_F\left[-\ln^2\frac{1-y}{y}-2\ln^2 z-2\ln\left(\frac{1-y}{y}\right)\ln z\right.$$

$$\left.-\tfrac{9}{2}\ln\frac{1-y}{y}-3\ln z-2\,\mathrm{Li}_2(u/y)-2\,\mathrm{Li}_2(1-z)\right]$$

$$+N_c\left[-\ln^2\frac{1-y}{y}-2\ln\left(\frac{1-y}{y}\right)\ln\omega\right.$$

$$\left.-2\,\mathrm{Li}_2(v/y)-\tfrac{11}{6}\ln\left(\frac{1-y}{y}z\right)-\tfrac{11}{6}\ln z\right]$$

$$+T_R\left[\tfrac{2}{3}\ln\left(\frac{1-y}{y}z\right)+\tfrac{2}{3}\ln z\right], \tag{A.3}$$

$$z=1-(1+\omega)(1-y),$$

$$u=y-(1-y)z,$$

$$v=y-(1-y)\omega,$$

$$\mathrm{Li}_2(x)=-\int_0^x\frac{\ln(1-t)}{t}\,\mathrm{d}t, \tag{A.4}$$

$$F_{12}=\sum_{i=1}^{5}f_i(\omega,y), \tag{A.5}$$

$$F_{13}=\sum_{i=6}^{10}f_i(\omega,y). \tag{A.6}$$

The functions f_i needed for the F_{12} are given below:

$$f_1(\omega,y)=C_F\left[\left(\frac{1-y}{y}\right)\left(\frac{z}{1-z}\right)-y+\frac{z}{(1-y)\omega}+\frac{1}{z}\right],$$

$$f_2(\omega,y)=\left(\ln\frac{1-y}{y}+\ln\omega\right)$$

$$\times\left[C_F\left\{4(1-y)+\frac{1-y}{z}\omega(2-y)\right\}+N_c\omega\frac{1-y}{z}\right],$$

$$f_3(\omega, y) = \ln(z)\Bigg[\frac{C_F}{(1-z)^2}\Big\{2\frac{(1-y)}{y^2}z^2(2-y) + z\omega\frac{1-y}{y^2}(4-3y)\Big\} + N_c\frac{z}{1-z}\Bigg],$$

$$f_4(\omega, y) = -2\big(C_F - \tfrac{1}{2}N_c\big)\Bigg[\frac{1}{(1-y)\omega z y}\big\{R(y_{12}, y_{23}) \times \big(z^2(1-y)^2 + y^2(1-z)^2\big) + R(y_{12}, y_{13})\big(z^2(1-y)^2 + z^2\big) + y/(y-(1-y)z)\big(\omega^2(1-y)^2 + z^2y^2\big)\big\} - 2\Big(\ln\frac{1-y}{y} + \ln z\Big)\Big\{\frac{(1-y)^2z^2}{(y-(1-y)z)^2} + \frac{2(1-y)z}{(y-(1-y)z)}\Big\}\Bigg],$$

$$f_5(\omega, y) = -N_c R(y_{13}, y_{23})\Big[\frac{1-y}{y}\omega/z + \frac{y}{1-y}z/\omega + 2/\omega\Big], \tag{A.7}$$

where

$$R(x, y) = \ln x \ln y - \ln x \ln(1-x) - \ln(y)\ln(1-y), \tag{A.8}$$

$$y_{12} = \frac{1-y}{y}z, \qquad y_{13} = \frac{1-y}{y}\omega, \qquad y_{23} = z. \tag{A.9}$$

The functions f_ι ($\iota = 6, \ldots 10$) for the F_{13} are given below:

$$f_6(\omega, y) = C_F\Big[\Big(\frac{1-y}{y}\Big)\Big(\frac{\omega}{1-z}\Big) + (1-y)\omega/(y-(1-y)z) + y/(1-y)z + 1/z - 2\Big],$$

$$f_7(\omega, y) = (\ln((1-y)/y) + \ln z)\Big[C_F y^2/u^2\big\{2((1-y)/y)^2\omega(2\omega+z) + ((1-y)/y)z(4\omega+z)\big\} + N_c(1-y)z/u\Big],$$

$$f_8(\omega, y) = \ln(z)\Big[C_F/(1-z)^2\big\{4\omega(\omega+z)((1-y)/y)^2 + ((1-y)/y)z(2\omega+z)\big] + N_c z/(1-z)\Big],$$

$$f_9(\omega, y) = -2\big(C_F - \tfrac{1}{2}N_c\big)\Big[1/(y(1-y)z^2)\big\{R(y_{12}, y_{23}) \times \big(\omega^2(1-y)^2 + y^2(1-z)^2\big) + R(y_{12}, y_{13})\big(\omega^2(1-y)^2 + u^2\big)\big\}$$

$$+1/[(1-y)(y-\omega(1-y))]\big((1-y)^2+y^2\big)$$

$$-2(\ln((1-y)/y)+\ln\omega)\big((1-y)^2\omega^2\big)/[y-\omega(1-y)]^2$$

$$+2(1-y)\omega/[y-\omega(1-y)])],$$

$$f_{10}(\omega, y) = -N_c[((1-y)/y)+y/(1-y)+2\omega/z^2]\,R(y_{13}, y_{23}). \qquad \text{(A.10)}$$

The function $R(x, y)$ is defined in (A.8). However, *note* that the variables y_{ij} for $f_6 - f_{10}$ are defined as

$$y_{12} = \omega(1-y)/y, \qquad y_{13} = z(1-y)/y, \qquad y_{23} = z. \qquad \text{(A.11)}$$

References

[1] C Basham, L Brown, S Ellis and S Love, Phys Rev Lett 41 (1978) 1585, Phys Rev D19 (1979) 2018, D24 (1981) 2382
[2] PLUTO Collaboration, Ch Berger et al, Phys Lett 99B (1981) 292
[3] A Ali and F Barreiro, Phys Lett 118B (1982) 155
[4] D G Richards, W J Stirling and S D Ellis, Phys Lett 119B (1982) 193, Nucl Phys B229 (1983) 317
[5] MARK-II Collaboration D Schlatter et al, Phys Rev Lett 49 (1982) 251,
MARK-J Collaboration B Adeva et al, Phys Rev Lett 50 (1983) 2051,
CELLO Collaboration H J Behrend et al, DESY report 82-022 (1982),
MAC Collaboration, (private communication)
[6] W A Bardeen, A J Buras, D W Duke and T Muta, Phys Rev D18 (1978) 3998
[7] G Sterman and S Weinberg, Phys Rev Lett 39 (1977) 1436
[8] A J Buras, 1981 Int Symp on Lepton and photon interactions at high energies (ed. W. Pfeil) p 636
[9] J Ellis, M K Gaillard and G G Ross, Nucl Phys B11 (1976) 253
[10] R K Ellis, D A Ross and A E Terrano, Phys Rev Lett 45 (1980) 1226, Nucl Phys B178 (1981) 321
[11] G C Fox and S Wolfram, Phys Rev Lett. 41 (1978) 1581, Nucl Phys B149 (1979) 413
[12] K Fabricius, I Schmitt, G Schierholz and G Kramer, Phys Lett 79B (1980) 431, Z Phys C11 (1982) 315,
F Gutbrod, G Kramer and G Schierholz, DESY report 83-044 (1983)
[13] Z Kunszt, Phys Lett 99B (1981) 429
[14] A Ali, J Korner, G Kramer, Z Kunszt, G Schierholz and J Willrodt, Phys Lett 82B (1979) 285, Nucl Phys B167 (1980) 454
[15] A Reiter, Univ of Heidelberg report HD-THEP-81-10 (1981)
[16] M Dine and J Sapirstein, Phys Rev Lett 43 (1979) 668,
K G Chetyrkin, A L Kataev and F V Tkachov, Phys Lett 85B (1979) 277,
W Celmaster and R J Gensalves, Phys Rev Lett 44 (1980) 560
[17] J C Collins and D E Soper, Nucl Phys B193 (1981) 381, B197 (1982) 446
[18] B L Ioffe, Phys Lett 78B (1978) 277
[19] A Ali, E Pietarinen, G Kramer and J Willrodt, Phys Lett 93B (1980) 155
[20] R D Field and R P Feynman, Nucl Phys B136 (1978) 1
[21] G Altarelli and G Parisi, Nucl Phys B126 (1977) 298
[22] S D Ellis, Phys Lett 117B (1982) 333
[23] T Sjostrand, LUND report LU-TP-82-3 (1982) and references therein
[24] PLUTO Collaboration Ch Berger et al, Z Phys C12 (1982) 297
[25] P B Mackenzie and G P Lepage, Phys Rev Lett 47 (1981) 1244, AIP Conf Proc 74 (1981) 176
[26] M R Pennington, R G Roberts and G G Ross, DTP/83/10 (1983)
[27] Talks at EPS meeting, Brighton, July 1983